ORGANIZATION OF ACETYLCHOLINE RECEPTORS IN QUICK-FROZEN, DEEP-ETCHED, AND ROTARY-REPLICATED *TORPEDO* POSTSYNAPTIC MEMBRANE

J. E. HEUSER and S. R. SALPETER

From the Department of Physiology, University of California School of Medicine, San Francisco, California 94143

ABSTRACT

The receptor-rich postsynaptic membrane of the elasmobranch electric organ was fixed by quick-freezing and then viewed by freeze-fracture, deep-etching, and rotary-replication. Traditional freeze-fracture revealed a distinct, geometrical pattern of shallow 8.5-nm bumps on the E fracture-face, similar to the lattice which has been seen before in chemically fixed material, but seen less clearly than after quick-freezing. Fracture plus deep-etching brought into view on the true outside of this membrane a similar geometrical pattern of 8.5-nm projections rising out of the membrane surface. The individual projections looked like structures that have been seen in negatively stained or deep-etched membrane fragments and have been identified as individual acetylcholine receptor molecules. The surface protrusions were twice as abundant as the large intramembrane particles that characterize the fracture faces of this membrane, which have also been considered to be receptor molecules. Particle counts have always been too low to match the estimates of postsynaptic receptor density derived from physiological and biochemical studies; counts of surface projections, however, more closely matched these estimates. Rotary-replication of quick-frozen, etched postsynaptic membranes enhanced the visibility of these surface protuberances and illustrated that they often occur in dimers, tetramers, and ordered rows. The variations in these surface patterns suggested that in vivo, receptors in the postsynaptic membrane may tend to pack into "liquid crystals" which constantly appear, flow, and disappear in the fluid environment of the membrane. Additionally, deep-etching revealed a distinct web of cytoplasmic filaments beneath the postsynaptic membrane, and revealed the basal lamina above it; and delineated possible points of contact between these structures and the membrane proper.

KEY WORDS postsynaptic receptors · membrane surfaces · cytoplasmic filaments · quick-freezing · deep etching

Tissue that has been quick-frozen is amenable to a new technique of viewing which is described in the following report. This technique is an amalgam of currently used electron microscope procedures which are only slightly modified to fit together. The final view presents membranes and filaments, and their interrelationships, in high-magnification, three-dimensional photomicrographs at the reso-

J. CELL BIOLOGY © The Rockefeller University Press · 0021-9525/79/07/0150/24 $1.00
Volume 82 July 1979 150–173

lution currently attainable on thin metal replicas (2 nm). Particularly valuable is the opportunity to observe in such replicas the overall organization of molecules associated with membranes—either individual molecules floating in the bilayer of the membrane or complex structural molecules comprising the cell cytoplasm beneath the membrane, or the extracellular coat outside. This is accomplished by deep-etching (i.e., shallow freeze-drying) of tissues that have been frozen in the absence of cryoprotectants. Cryoprotectants cannot be used because they do not etch away during freeze-drying. Thus it becomes difficult to avoid bad ice crystal formation during freezing. One way it can be avoided is by freezing at very high rates—by cooling at >20,000°C/s—which can be done with the freezing machine recently designed to capture synaptic vesicle exocytosis (38). Other rapid biological processes can now be viewed in this new way as well.

The problems that remain with this new viewing technique, besides the difficulty in freezing fast enough, are: (*a*) that etching leaves behind salts and other soluble components of the tissues, and these limit the final depth of etching and partly obscure the view; and (2) that the metal replica is produced in what is fast-becoming an old-fashioned Balzers' vacuum evaporator by depositing platinum and carbon onto tissue at a relatively warm temperature (−100°C). Cooling the tissue closer to 0°K would produce much finer grain replicas, but further cooling would cause severe contamination of the tissue surfaces by condensation of the residual gases that persist in the relatively poor vacuum obtainable in a standard Balzers'. Thus, further clarity of view must await better vacuum systems in which finer grain metals can be evaporated onto tissues held at lower temperatures (1, 8, 32).

The tissue first viewed by this method is the electric organ of *Torpedo*, a tissue composed almost entirely of acetylcholine-secreting nerve terminals and chemically excitable electric cells. The postsynaptic membranes of these electrocytes are already known to display an unusually high concentration of intramembrane particles when they are split apart and platinum-shadowed by standard freeze-fracture techniques (2, 17, 20, 56, 66). At other cholinergic synapses, such collections of intramembrane particles have been found especially in regions that bind α-bungarotoxin (α-BTX) (5, 25, 27, 34, 37, 58, 65, 68), a snake neurotoxin which is known to bind specifically to the acetylcholine receptor (43, 63). Thus the particles have been thought of as freeze-fracture views of the acetylcholine receptor molecules. Because the receptors are proteins which are known to form transmembrane ion channels when exposed to acetylcholine (4, 44, 57, 61), their appearance as particles in freeze-fracture replicas would be consistent with the widely accepted ideas that particles represent membrane proteins (12, 13).

One problem with the notion that the freeze-fracture particles represent cholinergic receptors has been that the concentration of particles per square micrometer is much less than the estimated density of receptor molecules.[1] A possible explanation for this discrepancy has recently been hinted at by Cartaud et al., who obtained views of the true external surface of this postsynaptic membrane by deep-etching isolated membrane vesicles purified from *Torpedo* electric organ (16, 17). Such vesicles were extremely enriched in cholinergic receptor proteins (21, 70), and, after freeze-etching, they appeared to be studded all over their surfaces with tiny, 8- to 9-nm flat-topped particles which often packed into tight hexagonal arrays where they reached concentrations in excess of 10,000/μm^2. Cartaud's platinum replicas of these surface structures looked very much like the negative-stain images of isolated cholinergic receptors (3, 16, 17, 55, 67), so naturally he interpreted these structures to be external views of the acetylcholine receptor molecules (17). He did not consider the problem, however, of why there are more of these surface

[1] Estimates of receptor density have been obtained in two ways. First, physiological recordings of the maximum postsynaptic membrane conductance produced by applying a saturating dose of acetylcholine have been compared to the best measurements of the individual acetylcholine channel conductance (4, 44, 57) to yield an estimate of 10,000 channels/μm^2. Second, quantitative autoradiography of saturable ^{125}I α-BTX binding to the postsynaptic membrane (27, 68) (which yields 21,000 ± 3,000 α-BTX binding sites/μm^2, according to recent corrections provided by M. Salpeter) has been compared with the best current estimates of how many α-BTX molecules bind to a single receptor (which is now generally thought to be 2 toxins/43, 63, 70), to yield an estimate that is also ~10,000 receptors/μm^2. In comparison, the reported concentration of intramembrane particles in the postsynaptic membrane of the cholinergic synapse has been reported to be between 3,000 and 6,000/μm^2, depending on the laboratory and the particular method of freeze-fracture (2, 17, 20, 39, 56, 58, 64, 66). This is 2–4 times less than the estimates of acetylcholine receptor density.

structures than there are intramembrane particles on the fracture faces of this same membrane.

A clue to understanding this problem has been provided by closer looks at the external fracture leaflet. This E face (13), in addition to displaying a low density of intramembrane particles, shows a subtle "roughness" which several observers have described as myriads of tiny particles that are ordered in some sort of geometrical array or lattice (20, 56, 66). Unfortunately, the values reported for the size and spacing of these structures in their lattice have been so small (6–7 nm) that it has been impossible to understand how they relate to the surface structures seen by Cartaud et al., or to the more typical fracture-face particles found within these membranes.

In the present report, we use quick-freezing to stabilize the molecular architecture of the postsynaptic membrane in the electric organ, and then use the new procedure of deep-etching, rotary-shadowing, and three-dimensional viewing of electron microscope negatives to examine true membrane surfaces and compare them with the membrane's two fracture-faces. By means of this approach, we reach several conclusions which reconcile the various views obtained by earlier investigators.

MATERIALS AND METHODS

Quick-Freezing

Tiny pieces of tissue were snipped out of the electric organs of small *Torpedo californica* or *Narcine braziliensis* under MS 222 anesthesia and immediately quick-frozen by slamming them against an ultrapure block of copper cooled to 4°K. The design and operation of the apparatus used for freezing have been described elsewhere (35, 38, 40). The apparatus performs high-speed impedance measurements at the time of tissue impact to ensure that the rate of cooling exceeds 20,000°C/s and that the surface of the tissue freezes in <1 ms.

Homogenization

Other pieces of tissue were gently sheared apart in 10 vol of distilled water containing 2 mM EGTA and 2 mM *N*-2-hydroxyethylpiperazine-*N'*-2-ethane sulfonic acid (HEPES) buffer, pH 7.2, by four up-and-down strokes in a Kontes-duall homogenizer (Kontes Co., Vineland, N.J.) with a loosely fitting Teflon pestle rotating at 50 rpm. We have shown previously that this treatment shears the electrocytes into broad sheets of innervated and noninnervated plasma membrane surfaces (36), as can be seen by comparing Figs. 1 and 2 with Figs. 3 and 4. These membrane sheets were immediately pelleted by a brief spin at 10,000 *g* and washed once more by resuspension and pelleting in the same distilled water medium. Then the pellets were mounted on the freezing machine and frozen in the same way as intact samples. This produced frozen samples of electric organ membranes which were essentially free of intracellular and extracellular salts and were thus particularly suitable for deep-etching. Postsynaptic membranes are easy to distinguish from other membrane fragments in the frozen homogenates because the nerve terminals remain attached throughout (Fig. 4). However, the absence of salt made these samples particularly prone to form large ice crystals as they froze, so quick-freezing with our liquid-helium-cooled machine became mandatory.

Exposure to Drugs and Fixatives

In an effort to visualize the receptor in the "open-channel" condition, small pieces of tissue or pellets of homogenates were soaked in 2×10^{-6} g/ml prostigmine for 15 min to block acetylcholinesterase, and then exposed to 10^{-4} M acetylcholine chloride for 10 s before quick-freezing. Other pieces of tissue were soaked in 10^{-4} M carbachol for 10 s before freezing. With such brief saturating doses of cholinergic agonists, more than half of the receptors should have been "open," yet few should have become desensitized (C F. Stevens, personal communication). In an effort to visualize receptors in the densensitized state, the exposure to 10^{-4} acetycholine or 10^{-4} carbachol was continued for 15 min before freezing. Finally, to serve as controls, other pieces of tissue were soaked in 10^{-5} M D-tubocurarine for 15–30 min before quick-freezing, to make sure the receptors were "shut."

For comparison with the quick-frozen samples, electric organs were taken from two fish that had been chemically fixed by rapid perfusion through the heart with 2% formaldehyde and 2% glutaraldehyde in a buffered medium made isotonic with elasmobranch blood. Tiny fragments from these fixed organs were soaked in 22% glycerol in elasmobranch Ringer's for 1 h, mounted on gold carriers, and frozen in the traditional way by immersion in Freon 22 cooled with liquid nitrogen. Other prefixed fragments were washed in distilled water, quick-frozen, and then fractured and deep-etched for comparison with the fresh homogenates that had been washed in distilled water.

Freeze-Fracture and Etching

All these frozen samples were stored in liquid nitrogen until transfer into a Balzers' 301 freeze-fracture machine (Balzers Corp., Nashua, N.H.). There they were fractured through the most superficial 10-μm thick region of good freezing by gently scraping the surface with a new ultrasharp razor blade mounted in the freezing microtome. The vacuum at time of fracture was $\geq 2 \times 10^{-6}$ torr and the tissue temperature was −120°C. At this point, some samples were etched for 3 min at −100°C and others were not. Some were replicated with a 2-nm thick layer of platinum-carbon (a change of 0.22 kHz on the quartz

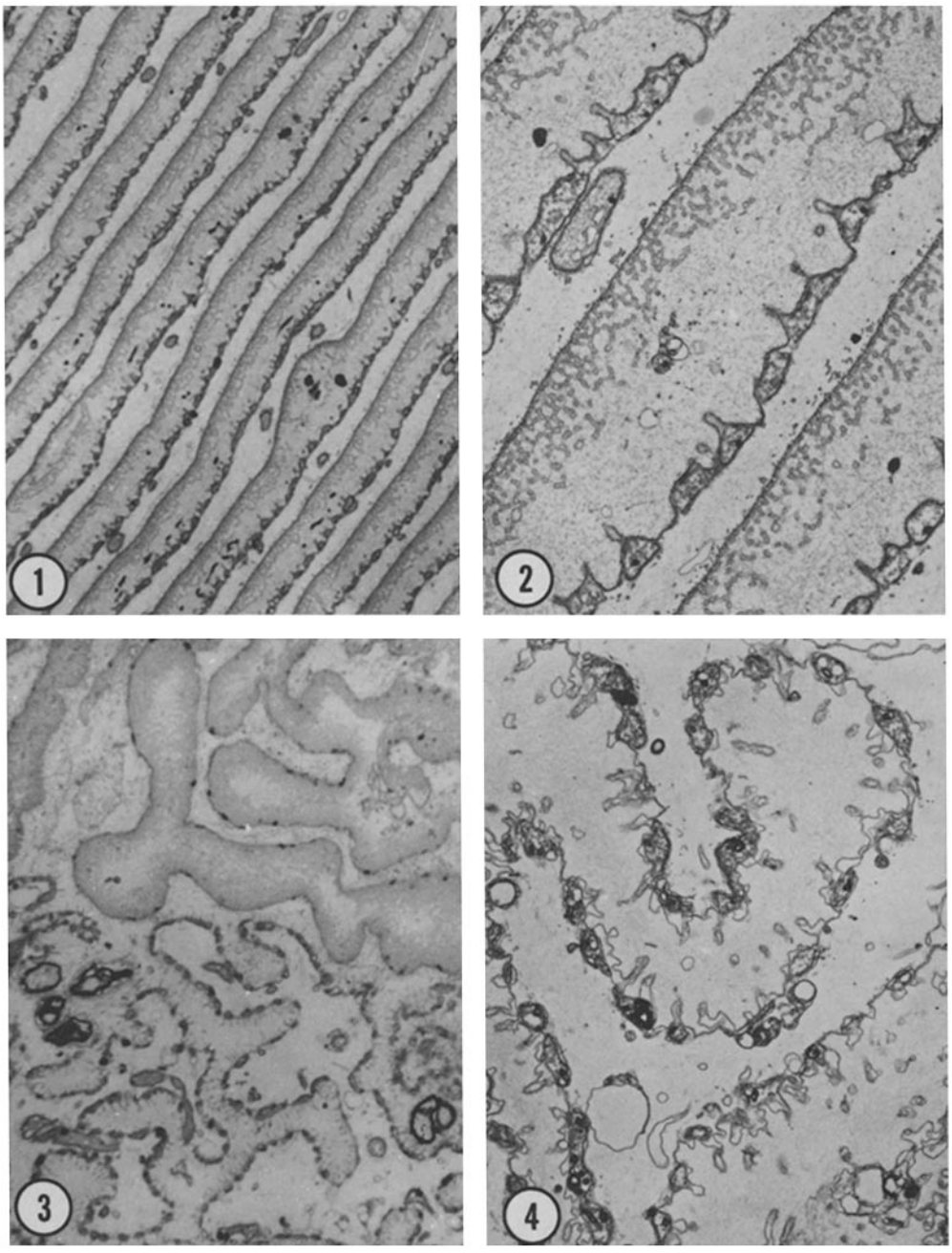

FIGURE 1 Light micrograph of a ¼-μm section through the electric organ of *Torpedo*, showing several flat electrocytes stacked on top of each other. × 1,000; so 1 mm = 1 μm.

FIGURE 2 Electron micrograph of the same field illustrates that each electrocyte is studded with nerve processes along its ventral surface. The dorsal surface of each cell displays myriads of deep, branching invaginations. The intervening cytoplasm contains wisps of material which are not visible at this low magnification. × 4,000; so 1 cm = 2.5 μm.

FIGURE 3 A light micrograph of a section through the low-speed pellet of the tissue fragments produced by gentle homogenization of electric organ. The electrocytes are sheared apart, but their plasma membranes hold together to form the convoluted profiles seen in the pellet. Nerve terminals still cling to the postsynaptic fragments, giving them a "beaded" appearance. × 1,000; so 1 mm = 1 μm.

FIGURE 4 Low power electron micrograph of the same pellet confirms cell disruption, but illustrates continuity of broad sheets of postsynaptic membrane and presence of relatively intact nerve terminals. × 4,000; so 1 cm = 2.5 μm.

crystal monitor) deposited with an electron beam gun mounted at 45° to the tissue surface, and operated at 2,050 V and 70 μA beam current. Others were rotary-replicated (49) with the new Balzers' rotary-stage attachment. In this case, the electron beam gun was mounted very flat, at 16–24° relative to the tissue surface, and operated at 2,050 V and 70 μA for 6 s, during which time the tissue was rotated through 360° six times. Both unidirectional- and rotary-replicas were backed with carbon deposited by 5–7 s of thermionic evaporation from pointed carbon rods.

Replicated tissues were removed from the Balzers' to a plastic scintillation bottle of frozen methanol which was allowed to thaw and "freeze-substitute" the tissue at the same time. This helped keep the replica intact. Then tissues were rinsed once in water and submerged in standard household bleach (sodium hypochlorite). The replicas floated off the tissue in the first few seconds of immersion in bleach and did not roll unless too much carbon backing had been deposited. They were then broken into grid-sized pieces which were individually transferred through two rinses of water in 10-ml dishes and picked up on 75-mesh Formvar- and carbon-coated grids. (Carbon was applied to the back of the grids to prevent them from becoming hydrophobic.)

Microscopy and Photography

Replicas were photographed at × 50,000 in a JEM 100C electron microscope operated at 80 kV with a 50-μm objective aperture. Stereo microscopy was performed with the high-resolution top-entry goniometer of a JEM 100B electron microscope by tilting the grid ± 6°. Electron microscope negatives were routinely contact-reversed in a homemade automatic device so that they could be printed as both positive and negative images. The negative images (in which platinum looks white and the shadows are black) were in general much more informative and have been used throughout this paper.

Particle sizes were measured on prints at ×200,000 using a 10× micrometer eyepiece. Only particles with complete shadows were used, and the diameters were measured across the interface between platinum and shadow (cf. references 1, 8, and 52).

RESULTS

Tissue Organization

Survey light microscope views such as Fig. 1 illustrated that the electric organ was composed of flat electrocytes stacked like coins to form a series battery capable of producing high voltages. The lower surface of each electrocyte was seen to be covered with tiny nerve branches. Low-power electron micrographs such as Fig. 2 illustrated that the electrocytes were relatively empty cells, with highly invaginated dorsal plasma membranes and smoother ventral plasma membranes closely apposed by nerve terminals.

When the tissue was homogenized, the electrocytes were sheared apart and yielded large, convoluted expanses of these two membrane surfaces. Nerve terminals clung to what had been the ventral membranes of the electrocytes throughout this disruption and made these postsynaptic membrane fragments look like "strings of beads" in light micrographs such as Fig. 3. They could thus be distinguished easily from fragments of dorsal noninnervated plasma membrane which looked thick and velvety because of the myriads of minute invaginations that characterized this surface.

Low-power electron micrographs of the innervated membrane fragments illustrated a remarkable preservation of synaptic morphology; the nerve terminals still contained their synaptic vesicles, and postsynaptic membranes still displayed their characteristic tubular invaginations, which were a prominent feature in the electron micrographs of intact tissue such as Fig. 2. Such membrane fragments could be quick-frozen and compared to tissue prepared in a more conventional manner.

Conventional Freeze-Fracture

To establish a baseline for comparison, fragments of electric organs from fish that had been perfused with aldehydes were fractured by the standard double-replica technique and platinum shadowed in the conventional way. Fortunate breaks yielded broad expanses of the innervated surfaces of electrocytes such as Fig. 5. These illustrated the branching pattern of the nerve, which was seen to contact almost half of the cell surface. Between these nerve branches, and in regions where the nerves were fractured away, fracture faces of the postsynaptic membrane were visible. These displayed a complement of intramembrane particles similar to that which has been described before in chemically fixed electric organs. P-face views of the postsynaptic membrane (Fig. 6) displayed a high concentration of intramembrane particles (~5,000/μm^2) which were of rather uniform size (8–10 nm), and occasionally packed together into tight aggregates. E-face views of this same membrane (Fig. 7) displayed a relatively low concentration of such intramembrane particles (~500/μm^2), and a high concentration of shallow "pits" which appeared to correspond in distribution and packing to the aggregates of particles seen on the opposite face. However, as is typical in

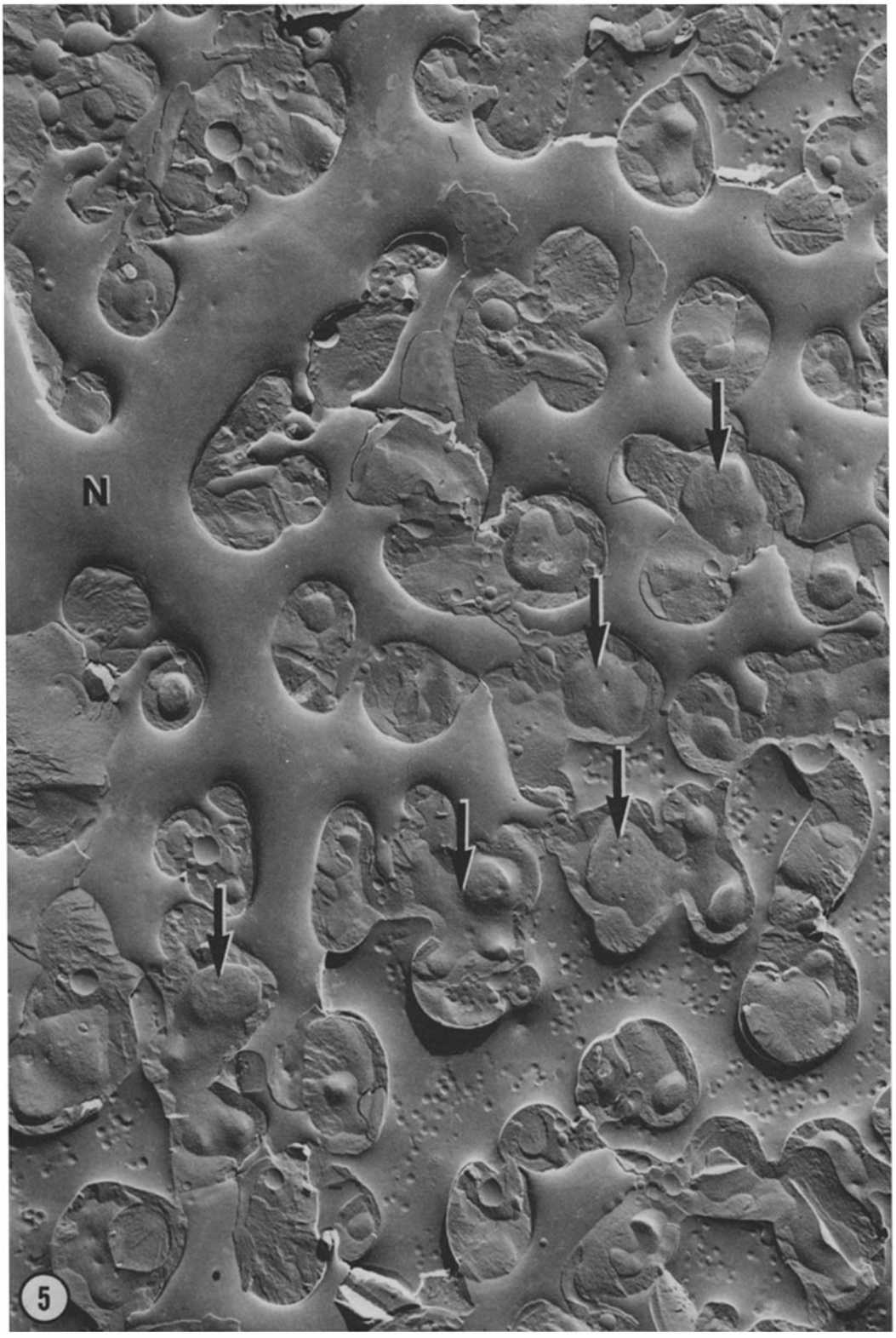

FIGURE 5 Survey view of the ventral surface of an electrocyte in a chemically fixed piece of *Torpedo* electric organ. Freeze-fracture has followed mostly the backside of the nerve arborization (*N*), but in the lower part of the field has followed its synaptic surface (which is peppered with bulging synaptic vesicle contacts resulting from the 20 mM magnesium in the fixative). Between nerve processes protrude gentle mounds in the postsynaptic membrane (arrows). These areas provided most of the postsynaptic membrane views presented in this report, but in fact represented the only "nonsynaptic" areas that existed in this membrane. × 13,000; so 1 cm = 0.75 μm.

freeze-fracture replicas, the E-face pits looked much smaller than the P-face particles.

Freeze-Fracture of Quick-Frozen Tissue

In contrast to this conventional image, postsynaptic membranes in small fragments of electric organ which were quick-frozen immediately after removal from anesthetized fish looked somewhat different. Micrographs such as Fig. 8, printed at the same magnification as the previous two, illustrated that in quick-frozen tissue intramembrane particles were less uniform in size and included many larger, irregular forms, a few of which looked like aggregates of two or more smaller particles. Moreover, the partitioning of these particles between the two membrane faces was less asymmetric than in fixed tissues. Though the P face still displayed the majority of intramembrane particles, micrographs such as Fig. 9 illustrated that the E faces of quick-frozen membranes displayed considerably more particles than they did in fixed tissues. This difference in particle partitioning between quick-frozen and fixed postsynaptic membrane has been observed before (40).

Another basic difference in the fracturing properties of fixed and frozen postsynaptic membranes could be readily appreciated by comparing micrographs of E faces of the two, such as Figs. 7 and 9. In quick-frozen tissue, the postsynaptic E faces displayed a rough-textured background behind the intramembrane particles, which itself appeared to be composed of very shallow bumps arranged in rows, quite unlike the clusters of shallow pits seen in chemically fixed tissues. The recent report by Cartaud et al. (17) displayed this difference between fixed and frozen E-face images as well.

Deep-Etching of Quick-Frozen Tissue

The tryptych of Figs. 10–12 compares the different views that could be obtained of postsynaptic membrane invaginations from three different freshly homogenized fragments of *Torpedo* electric organ, prepared in the same way as the ones in Fig. 3 and then quick-frozen. In Fig. 10, the frozen tissue was fractured and then immediately platinum-shadowed at 45° in the conventional manner. An E fracture-face similar to that in Fig. 9 was revealed, but the extracellular space above and the cytoplasm beneath the membrane were without obvious structure. In Fig. 11, the frozen tissue was etched for 3 min at −100°C after fracture, before platinum-shadowing. This lowered the water table enough to reveal the barbed-wire appearance of the basal lamina above the postsynaptic membrane in the synaptic cleft and to reveal a number of filaments in the etched cytoplasm beneath the postsynaptic membrane.

However, the structures revealed by etching were partly obscured by the deep shadows cast by evaporating platinum in the usual manner from a fixed 45° angle. This problem was alleviated, as seen in Fig. 12, by fracturing and etching for 3 min as before, but then coating the tissue uniformly with platinum by rotating it as the platinum was deposited (49), similar to what is done during gold coating for scanning electron microscopy. This eliminated the deep, dark shadows and highlighted the exposed cytoplasmic and extracellular structures with a thin layer of platinum.

Most fortunately, such rotary-shadowing also highlighted subtle surface details on portions of the postsynaptic membrane exposed by etching. Fig. 13 was one particularly fortunate exposure of what was unquestionably a view of the true external surface of the postsynaptic membrane. The surface was obscured on the left by an overlying network, identified as the basal lamina in planar view, and was broken through on the right to reveal filaments in what must have been the underlying cytoplasm. This interpretation of relative depths could be made relatively accurately, even by inexperienced observers, on such photographically reversed images as Fig. 13. But a more positive identification could be made by examining the stereo images in Fig. 14, printed the way the replica looked in the electron microscope, with platinum appearing black. The lower black hole (white in this case) was seen to be the mouth of an invagination in the postsynaptic membrane, leading away from the viewer and stuffed with a rind of basal lamina. (It is important to stress that stereo-pairs of freeze-etch replicas should not be viewed by crossing one's eyes and fusing the central image, because this actually reverses the sense of depth and makes the replica look inside out, or as if viewed from the backside. A pocket stereo viewer must be used.)

Outer Surface of Postsynaptic Membrane

The most striking feature of the true surface of the postsynaptic membrane viewed in Fig. 13 was the plethora of tiny protrusions that peppered it. These were individually small 8- to 9-nm deposits

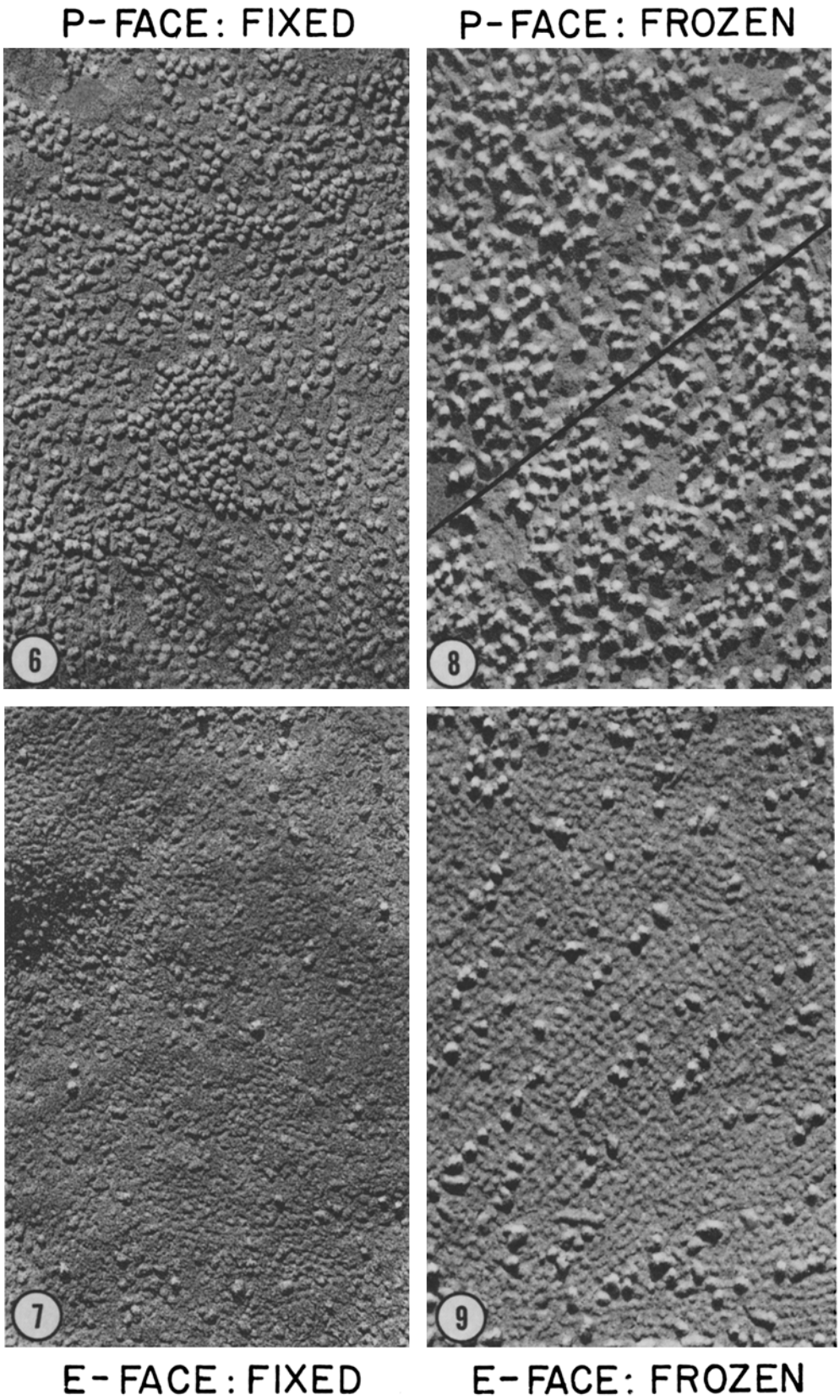

FIGURES 6–9 Comparisons between P and E fracture-faces of postsynaptic membranes from chemically fixed, glycerinated, and Freon-frozen tissue versus tissue quick-frozen immediately from the living state. All are printed at the same magnification to clarify the differences discussed in the text. × 165,000; so 1 mm = 6 nm.

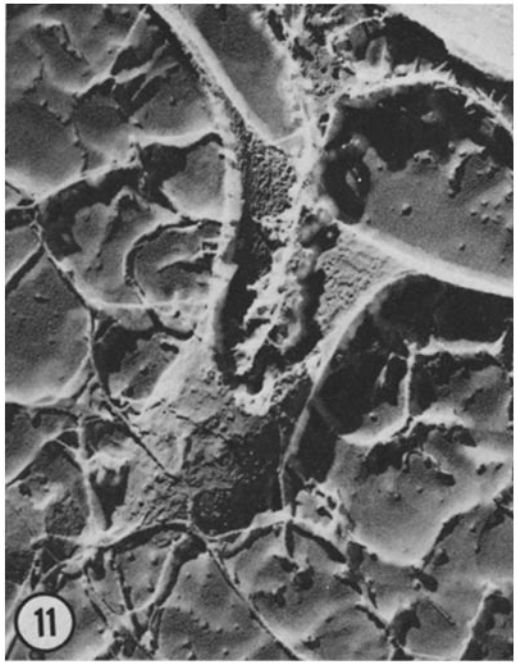

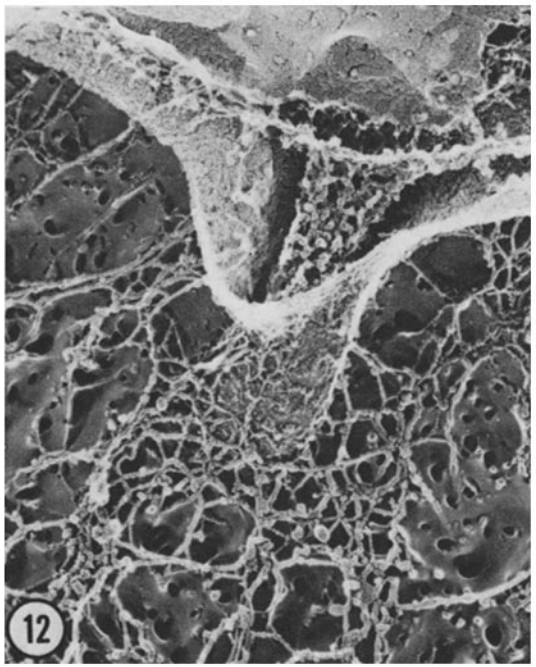

FIGURE 10 Postsynaptic membrane invagination in homogenized fragment of electric organ, seen after traditional freeze-fracture and 45° shadow-casting with platinum, without etching. × 88,000; so 1 cm ≃ 0.1 μm.

FIGURE 11 Similar postsynaptic membrane invagination in homogenized tissue, which was etched for 3 min at −100°C after fracture, and then replicated as in Fig. 10. × 55,000; so 1 cm ≃ 0.2 μm.

FIGURE 12 Similar postsynaptic membrane invagination fractured and etched as before, but then uniformly coated with platinum by the new technique of rotary replication (49). × 50,000; so 1 cm ≃ 0.2 μm.

of platinum. In many areas they occurred in groups of two or four, and so looked like tiny "molars." In other areas, they lined up in characteristic double-rows and these rows often occurred in pairs, making four rows abreast. Often, however, the surface protrusions occurred in more random aggregates. Their concentration was $>10{,}000/\mu m^2$ in most areas. They were presumably the same structures that Cartaud et al. (17) observed on the external surfaces of the excitable vesicles isolated from *Torpedo* electric organs.

The question immediately arose of the relation of these surface structures to intramembrane particles. No particles were seen in Fig. 13 because the membrane broke straight through to the cytoplasm. This was a characteristic of all quick-frozen tissue; there was much less tendency to fracture within membranes and much more cross-fracture. Also, those membrane fracture-faces that were produced in quick-frozen tissue tended to develop "pot holes" or collapsed completely during etching. Thus, it was easier to compare the surface protrusions with intramembrane particles on replicas of deep-etched samples of electric organ that had been prefixed with aldehyde, washed in distilled water, and then quick frozen. (The wash in distilled water after fixation removed the salts and facilitated etching considerably.) Fig. 15 was an area of postsynaptic membrane in such prefixed tissue which was topologically very similar to Fig. 13. On the far left, the (fixed) basal laminae overlay the membrane surface. In center left, the true membrane surface was seen, with the characteristic four-abreast alignments of 8- to 9-nm surface structures. (The protrusions did not form such neat rows in chemically fixed tissues, but displayed the same overall pattern of organization as in quick-frozen tissues.) Just to the right of this, the surface changed texture and the high density of aligned structures changed to a random scattering of more pleomorphic platinum aggregates. This was the rotary-replicated image of the P fracture-face; here the outer half of the membrane had been peeled away during fracture. To the far right, the inner half of the membrane with its P face was also torn away and the underlying cytoplasmic filaments were revealed (here somewhat coarsened by the aldehyde fixation).

The crucial interface zone between the true surface and P fracture-face, where the surface protrusions and intramembrane particles could be compared, was examined at higher magnifications such as that in Fig. 16. It was quite apparent that the surface structures were much more abundant and more strikingly organized than the adjacent intramembrane particles. Also, the surface protrusions appeared to be more uniform in height than the intramembrane particles, except along the immediate interface with the fracture-face where the surface structures often appeared considerably distorted (arrows).

Fig. 17 epitomized the appearance of the surface projections under the best circumstances of tissue preparation and viewing. This was from an experiment in which isolated postsynaptic membrane fragments were prepared in 0.1 M salt and quick-frozen as soon as was practical. In this case, a relatively thick layer of platinum was applied all around, so the surface projections looked like small "rings," not unlike the "doughnuts" seen after negative staining of this membrane. They were so distinct that it was easy to see the pattern of grouping into rows four abreast and the cracked variants thereof (arrow).

Comparison of Surface Structures with Fracture-Faces

This pattern was quickly thought to relate in some way to the subtle texture seen on E faces of unfixed postsynaptic membranes, described in relation to Fig. 9 above. The E face was, after all, the underside of the external leaflet of the membrane, out of which the projections extended. This E-face texture also appeared to be composed of rows of very shallow bumps, and upon close inspections of micrographs such as Fig. 18, printed at the same magnification as Fig. 17, it was clear that the E-face rows also occurred in groups of two or four abreast in which adjacent rows achieved the same close spacing (8–9 nm) as did the surface protrusions.

More quantitative evidence that surface protrusions and E-face lattice bumps were opposite sides of the same postsynaptic membrane components was obtained by measuring the sizes of all the particles in well-defined areas of each of the various views of the postsynaptic membrane. First, surface structures and P-face particles were measured on areas such as that in Fig. 15. When compared to each other (Fig. 19) surface structures were clearly smaller and more plentiful than P-face particles. Then, E-face structures were measured in areas such as Fig. 18. Those which stood out prominently above the surface and cast a long

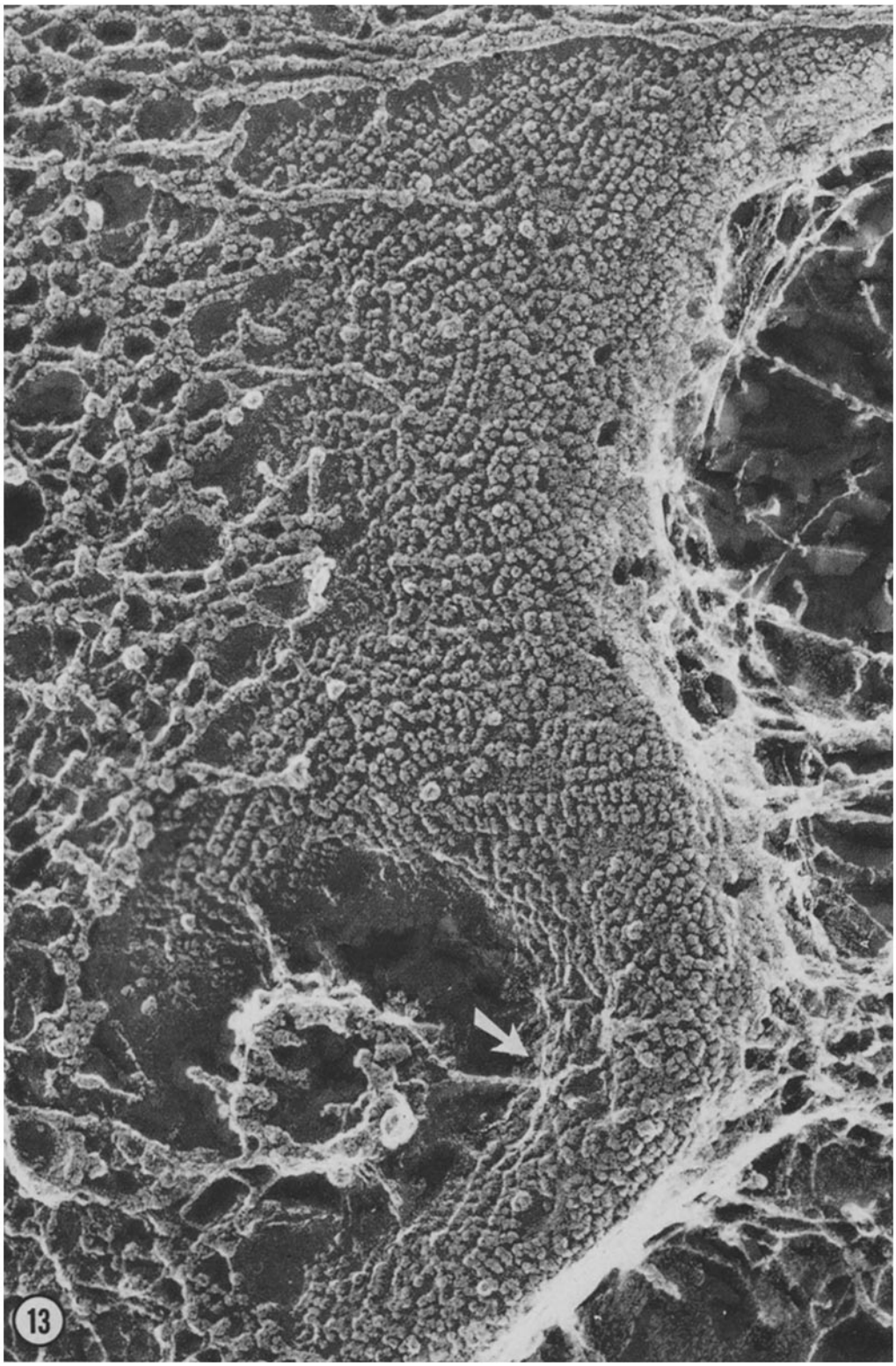
13

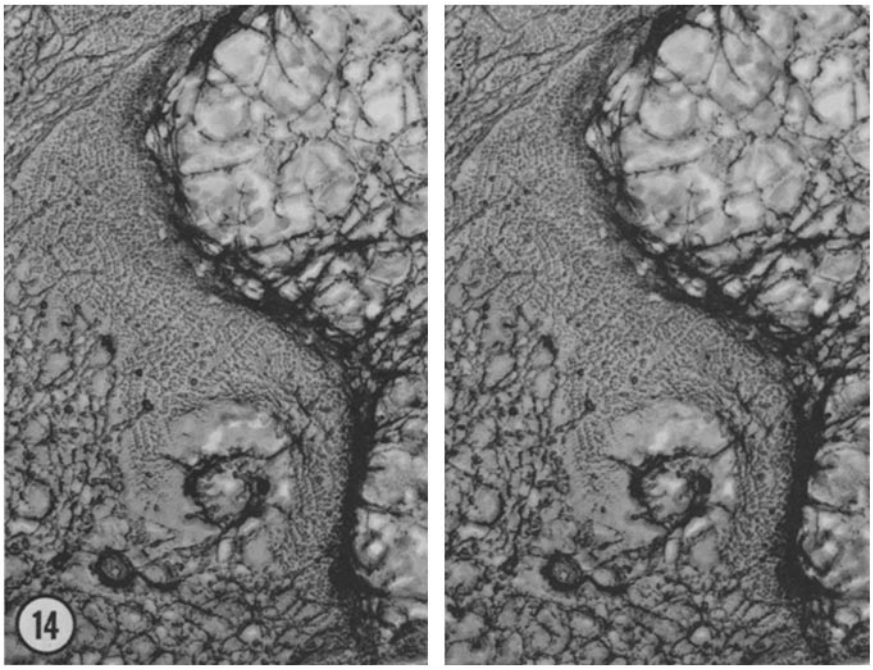

FIGURE 14 Three-dimensional view of the same field as in Fig. 13, displayed the way it actually looked in the electron microscope before photographic reversal. The platinum deposit which coated every surface irregularity as a result of rotary-replication looks black here instead of white, so the image is harder to interpret without the aid of a pocket three-dimensional viewer. × 60,000.

black shadow were considered "particles" and those which were shallower and grouped in rows were counted as "lattice" structures. When compared to each other in Fig. 20, it was clear that the lattice structures were also smaller and more numerous than the more prominent E-face particles. Comparing the two graphs showed that E-face particles were similar in size to P-face particles, and, more important, confirmed that the E-face lattice bumps were similar in size and concentration to the surface protrusions. Thus, it seemed logical to conclude that these two were opposite views of the same structure. This is diagrammed in Fig. 21, which also displays the added supposition that the larger, more prominent P- and E-face particles represented membrane-intercalated structures that pulled out of one membrane leaflet or the other during fracture.

Attempts to Alter Postsynaptic Membrane Structure

There was no apparent effect of acetylcholine on the structure or packing of the surface protrusions, nor on the fracturing properties of the postsynaptic membrane. It was impossible to distin-

FIGURE 13 Panoramic view of the postsynaptic membrane revealed by deep-etching a broken electrocyte and replicating it by rotary deposition of platinum. To the left, the lacelike basal lamina lies above the membrane and obscures it from view. Bottom center, this basal lamina assumes a ringlike appearance as it dips down into a dark postsynaptic invagination. Here and there, strands of the basal lamina extend out and attach to the postsynaptic membrane with clawlike feet (arrow). In the middle of the figure, the basal lamina has been fractured away to reveal the true external surface of the membrane. Because of rotary-replication, the clusters and linear arrays of 8- to 9-nm protrusions which characterize this surface can be seen very clearly. To the right, the postsynaptic membrane has broken through to reveal the underlying meshwork of cytoplasmic microtrabeculae (cf. 71) which gird it from beneath. × 175,000; so 1 mm ≃ 6 nm.

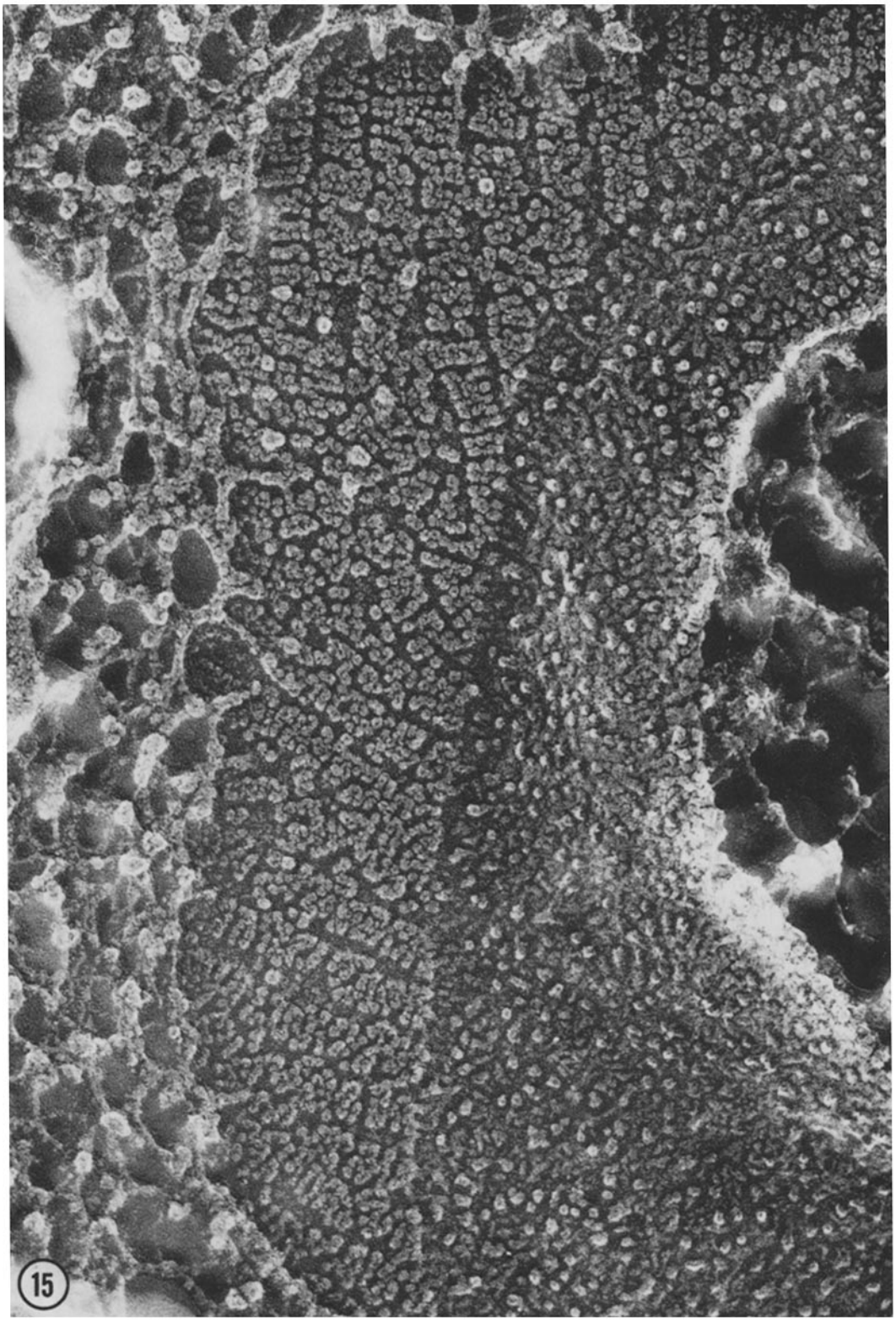

FIGURE 15 Deep-etched, rotary-replicated view of aldehyde-prefixed postsynaptic membrane, illustrating, from left to right, first the weblike basal lamina above the membrane, then the true surface of the membrane with its profusion of aligned surface projections, then the P fracture-face with a lower concentration of more randomly scattered intramembrane particles, and finally, on the far right, a break in the membrane which reveals underlying cytoplasmic trabeculae. × 200,000; so 1 mm ≃ 5 nm.

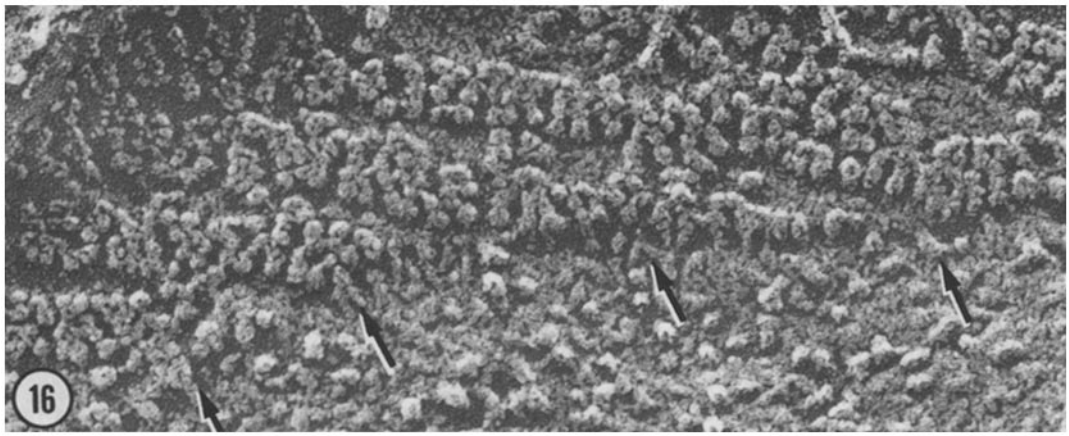

FIGURE 16 Higher magnification of the interface between true surface (above) and fracture-face (below) of the postsynaptic membrane, to contrast the appearance of surface projections and intramembrane particles. Surface projections located at the immediate interface with the fracture-face appear distorted (arrows). × 300,000; so 3 mm ≃ 10 nm.

guish membranes that had been soaked in 10^{-4} M acetylcholine for 10 s before freezing (or in 10^{-4} M carbachol, which was a more stable agonist) from those that had either not been soaked, or had been soaked in curare (10^{-5} M) for many minutes before freezing to block all acetylcholine action.

Moreover, it was not possible to distinguish membranes that had become "desensitized" by prolonged exposure (15 min) to 10^{-4} M acetylcholine or 10^{-4} M carbachol from untreated membranes. Thus, the structural differences between "open," "closed," or "desensitized" states of the receptor were too subtle to be detected in these platinum replicas.

Deep-Etching of the Cell Interior

Deep-etching of postsynaptic membrane fragments provided a wealth of other views of this isolated synapse preparation. Fig. 22 was a particularly attractive field in a unidirectional shadow-casting which showed a nerve terminal, on the right, fractured open and etched to reveal the synaptic vesicles inside. The terminal was spaced apart from the electrocyte by a veil-like basal lamina. Immediately to the left of the basal lamina, the underside of the postsynaptic membrane was visible, as it was in Fig. 11; and, again, cytoplasmic filaments could be seen to contact its inner aspect.

A very similar field was found in one of the early rotary-replicas of quick-frozen membrane fragments, and is displayed in Fig. 23 for comparison. The rotary deposition of platinum eliminated shadows and brought into higher contrast such internal cytoplasmic structures as synaptic vesicles in the nerve and filaments in the electrocytes. The photographic reversal made such structures white against a dark background, so that the image looks like a particularly high-resolution scanning electron micrograph, though it was produced in an ordinary transmission electron microscope.

Fig. 24 displays another synapse found in this particular replica. Here the nerve was not broken open to reveal its vesicles, but instead looked like a grey orb surrounded by a delicate veil of basal lamina, which separated it from the postsynaptic membrane. Here, etching had exposed a relatively large expanse of the true inner (cytoplasmic) surface of the postsynaptic membrane, which displayed more clearly the delicate web of cytoplasmic filaments which underlay the postsynaptic membrane. Stereo views of this inner aspect of the postsynaptic membrane (Fig. 25) demonstrated how deep the etching was—often 0.25 μm or more—and yet how little the etching had distorted the thin filaments that comprised the cytoplasmic web (cf. references 23, 45, and 71). (Again, Fig. 25 should not be viewed with crossed eyes, or else the invagination in the lower right corner of the field will look as though it is going away from the observer.)

Fig. 26 displayed at optimum magnification the organization of this postsynaptic web. It appeared to be a branched, interconnected mesh of filaments, each 5–10 nm thick. In this field, as in most

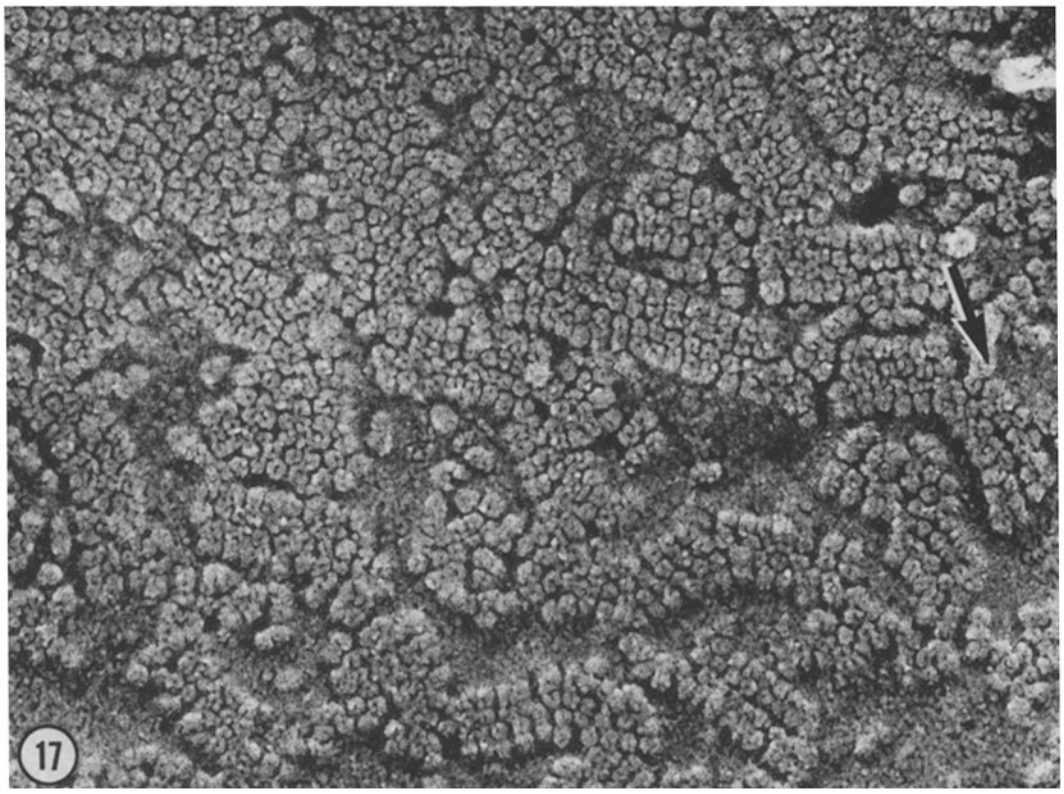

17

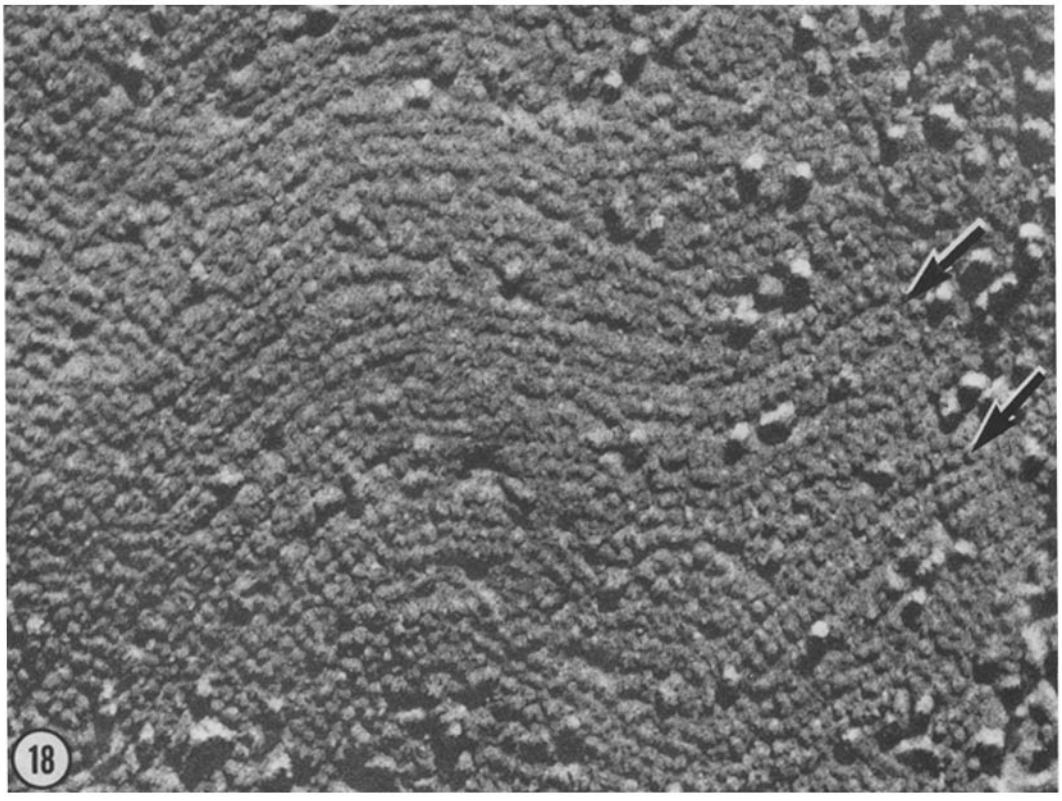

18

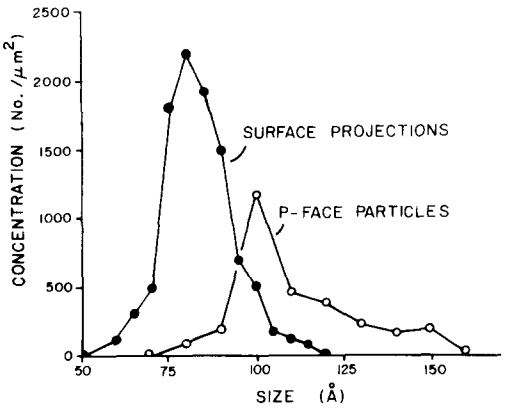

FIGURE 19 Size histograms of the projections on the true membrane surface versus the P-face intramembrane particles, to illustrate that the surface projections are smaller and more regular in size than the intramembrane particles.

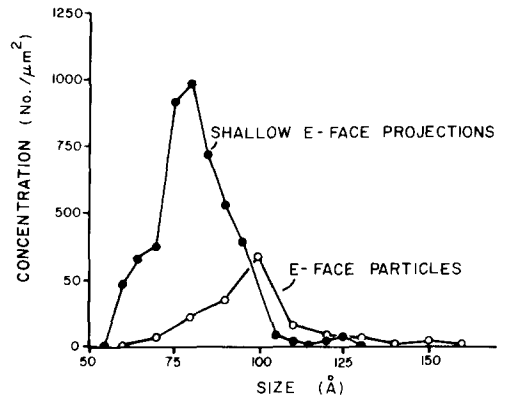

FIGURE 20 Size histograms of tall versus shallow particles seen on the E fracture-face, to illustrate that the shallower particles are significantly smaller and more numerous than the taller intramembrane particles and thus match the surface projections measured in Fig. 19.

freeze-etchings, the filamentous strands appear to run up to the postsynaptic surface and terminate. It was not clear what relation they had to the aforementioned protrusions seen on the opposite side of this membrane.

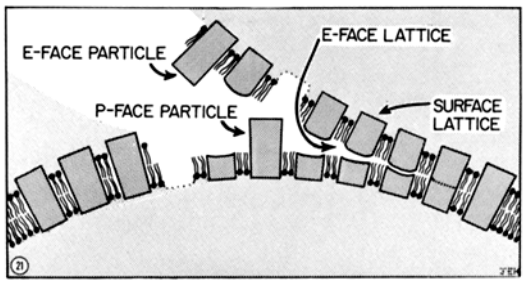

FIGURE 21 Diagram illustrating, first, how cleavage of intramembrane receptor molecules could generate the match between the E face lattice and the surface lattice of projections that is observed in etched *Torpedo* postsynaptic membrane; and second, how extraction of whole receptors from one leaflet or the other could generate the large intramembrane particles which also characterize this membrane.

So far, all attempts to decorate these filaments with the S_1 fragment of myosin have failed, so it is not possible to conclude that they are composed of actin. Nevertheless, electrocytes are embryologically derived from muscle cells and are known to be rich in contractile proteins (41). Thus, experiments along this line are continuing.

DISCUSSION

The preceding observations suggest that the tiny, ordered E-face "particles" seen by earlier investigators in chemically fixed *Torpedo* electrocyte membranes (20, 56, 66) correspond to the undersides of the surface structures that Cartaud et al. exposed by freeze-etching purified postsynaptic membrane vesicles (16, 17). There is a close correspondence when the two can both be seen in the same tissue, as after quick-freezing and the new viewing technique outlined here. On both sides of the membrane, these structures (*a*) appear to be of the same size (~8.5 nm) and are packed closely together, often at a density of $>10{,}000/\mu m^2$; (*b*) are aligned into long double rows, often into closely spaced pairs of double rows; and (*c*) look like the structures seen before in negatively stained

FIGURE 17 Characteristic view of the pattern of grouping of surface projections seen on deep-etched postsynaptic membrane fragments. The most obvious pattern is rows four abreast, with many breaks and curves (arrow). × 270,000; so 3 mm ≃ 10 nm.

FIGURE 18 Unidirectional shadow-casting of an unetched E face of the postsynaptic membrane, exposed by fracturing intact, quick-frozen tissue, which illustrates that the shallow bumps seen on this surface also group into curvilinear rows, most often two or four abreast (arrows), like the surface projections in Fig. 17. × 270,000; so 3 mm ≃ 10 nm.

fragments of postsynaptic membrane (3, 16, 17, 55, 67).

Previous investigators have argued that the ordered structures seen in such negatively stained or in deep-etched membrane fragments represented acetylcholine receptor molecules, largely because the membrane fragments had been purified to the point where they contained little else except this membrane protein. Thus, it is reasonable to presume that the patterned arrays of membrane structures seen here, in quick-frozen and deep-etched postsynaptic membrane *in situ*, also represent receptor molecules.

Fracturing Properties of the Cholinergic Receptor

The structures in question differ in one important respect, however, from what would be expected to result when membrane receptors were freeze-fractured. Though they extend quite far out into the extracellular space, as a receptor well might, they extend inward into the membrane interior only slightly more than halfway. That is, when viewed from inside the cell, they extend only a very short distance out of the E face. In fact, they are so shallow in this view that they were previously seen only faintly, and then only when the postsynaptic membrane happened to be shadowed at a very low angle which accentuated differences in elevations (17, 56, 66). Then, their size and spacing appeared to be only 7 nm, but that may have been because such obliquely shadowed membranes were tipped relative to the electron beam and thus their image was foreshortened.

It was difficult to actually measure how much the shallow E-face particles extended out of the background fracture plane in this material, but they clearly did not extend far enough to reach all the way through the postsynaptic membrane to the inside of the cell. Yet the receptor mediates a transmembrane ionophore (44, 67). This possibly indicates that the structures in question represent only the superficial portion of the molecular complexes that comprise receptors and ionophores in this membrane. If so, these molecular complexes would appear to be susceptible to fracture at a point about midway through the membrane, at about its hydrophobic center. This is diagrammed in Fig. 21. Possibly this could be a boundary between different molecular subunits.

Scattered among the shallow E-face structures were taller, more prominent intramembrane particles which could have spanned the whole width of the postsynaptic membrane before fracture. These large particles may have resulted when receptor molecules did not break near their middle but held together and pulled out of the internal leaflet of the membrane during fracture. Similarly, P-face particles would result when the molecules also held together but adhered to the inner half of the membrane more strongly and pulled their heads out of the external leaflet during fracture. Indeed, the P-face particles found in the postsynaptic membrane often looked sufficiently tall to extend all the way through the external leaflet and 5 nm into the extracellular space. (This was seen clearly in oblique views where the true surface lay adjacent to the P-fracture face, as in Fig. 16.) Indeed, some investigators have even been able to show that such P-face particles display small dimples at their apices, as do the surface structures seen after deep-etching or negative staining (2, 65). Thus, this theory of the origin of more traditional intramembrane particles has been included in the diagram of Fig. 21.

Because the concentration of surface protrusions was $\sim 10{,}000/\mu m^2$, while the concentration of normal intramembrane particles summed for both E and P faces totalled $\sim 5{,}000/\mu m^2$, it would appear that only about half of all the transmembrane structures hold together to produce prominent particles during fracture. This can explain way particle counts have always been less than half that expected from estimates of postsynaptic receptor density (27, 62, 65, 68).

Which receptors will hold together during fracture seems to be a random process unaffected by the behavior of neighboring structures, because histograms of intramembrane particle sizes showed that only a small proportion of the particles were large enough to be aggregates of two or three neighbors, and aggregates would be expected if the tenacity of one receptor helped a neighbor to hold together during fracture. The decision of whether to break or not, and which face to stick to during fracture, also did not appear to be affected by applying agonists or antagonists to the membrane in the moments before freezing, because such treatments changed neither the concentration, nor the size, nor the partitioning of intramembrane particles.

It is puzzling that the intramembrane particles were usually larger and more irregular in quick-frozen tissue than were the surface protrusions, if

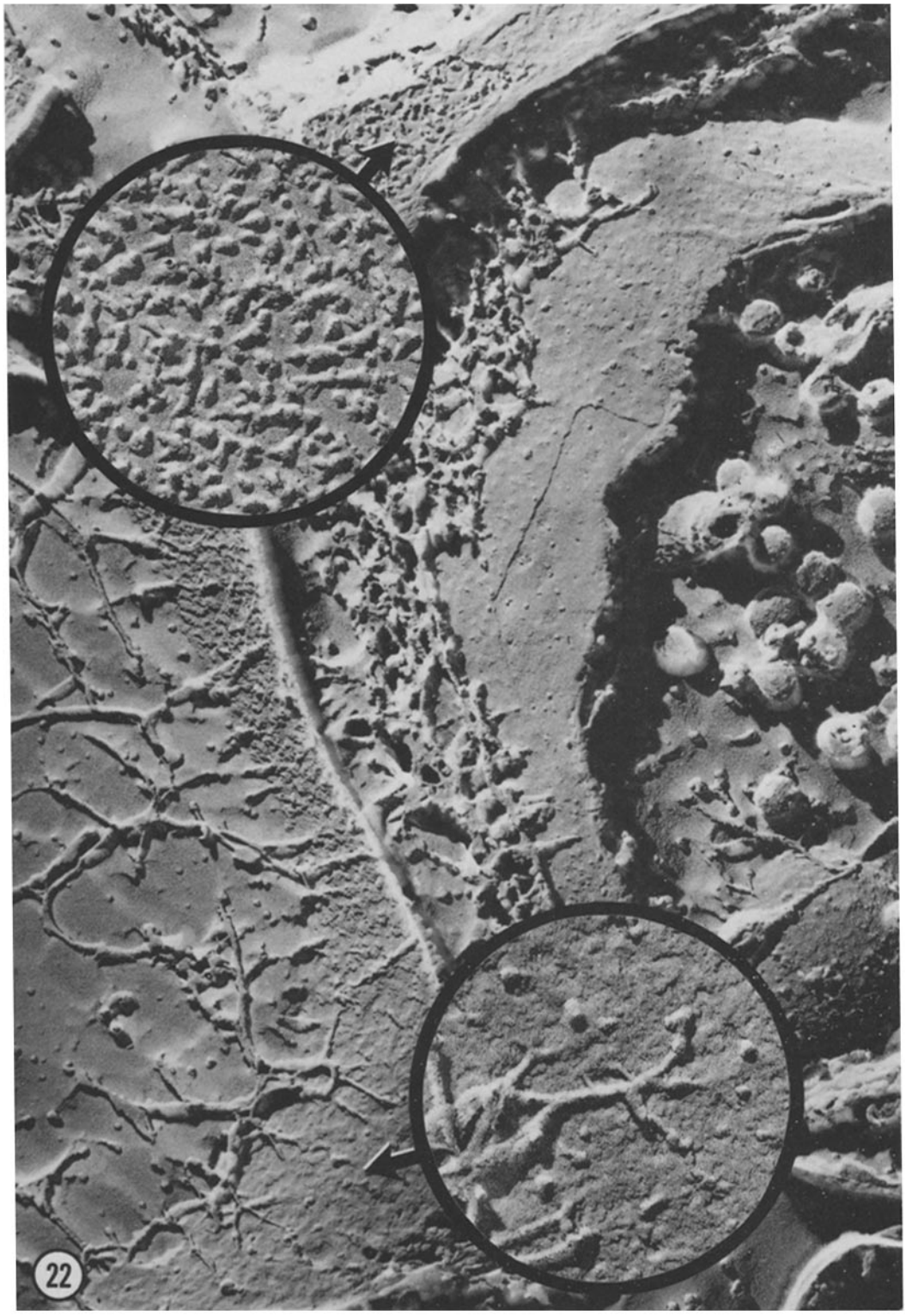

FIGURE 22 Panoramic view of an electric organ synapse in deep-etched, unidirectionally shadowed material, seen from a vantage point within the postsynaptic cell. To the left is electrocyte cytoplasm containing its characteristic web of filaments. These are seen to insert into the underside of the postsynaptic membrane (lower *inset*). The upper crescent of the postsynaptic membrane has been fractured and reveals the irregular intramembrane particles which characterize this membrane's E face after quick freezing (upper *inset*). The center of the figure provides an oblique view through the synaptic cleft in which the veil-like basal lamina has been exposed. To the right is the nerve terminal, inside of which can be seen several synaptic vesicles and a few axoplasmic filaments. × 75,000; *insets* × 200,000.

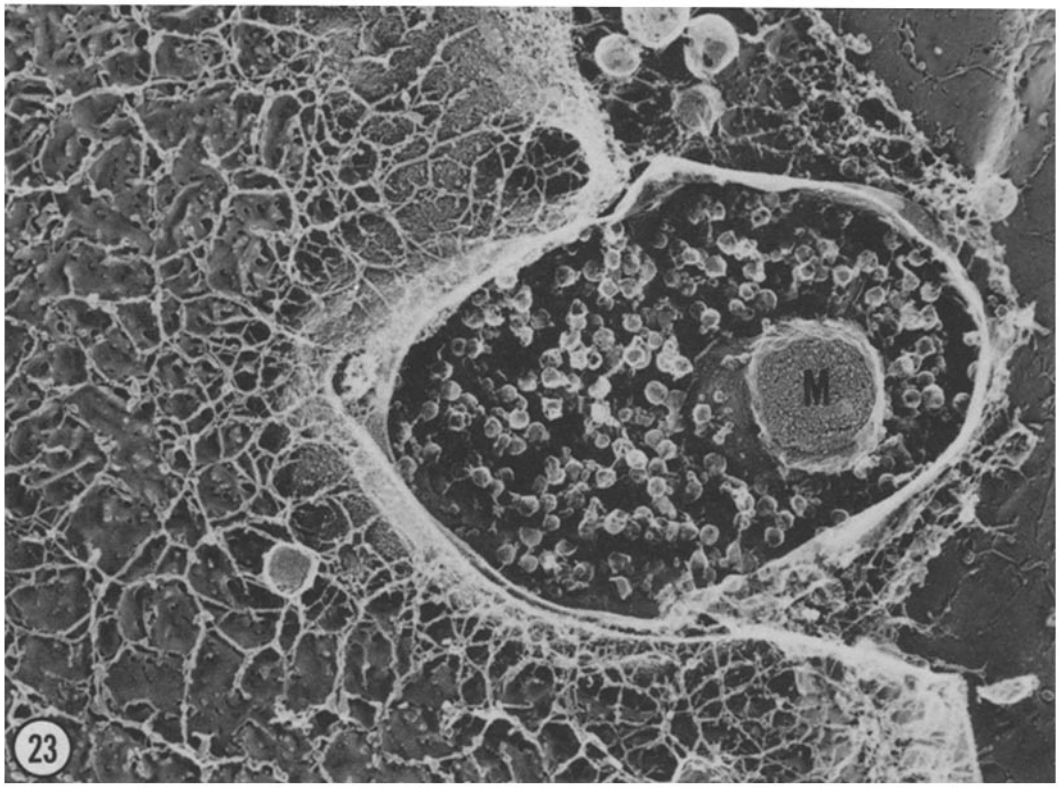
M
23

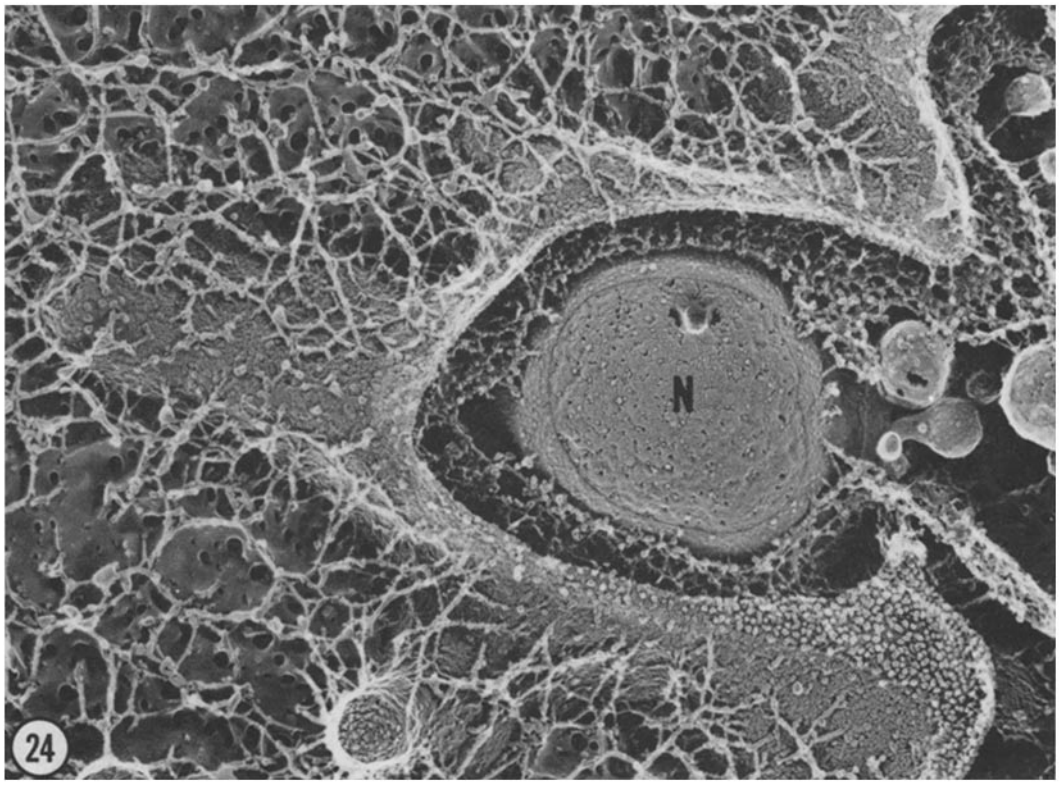
N
24

both were, in fact, different views of the same structures. Possibly this was due to distortion of the molecules when they pulled out of one membrane face during fracture, or to decoration and enlargement of the exposed molecules by nonuniform condensation of either residual gases from the vacuum or of the platinum itself during evaporation (1, 8, 32). Alternatively, the relatively larger size of intramembrane particles may have been a result of partial collapse of the monolayer of lipids surrounding them in the course of etching or replication (15). In any case, the relative uniformity in the size and shape of surface protrusions suggested that they were a more accurate indication of the original size of the postsynaptic receptor molecules.

The Pattern of Receptor Organization in the Plane of the Membrane

The question naturally arose of whether the pattern seen on the surface of this membrane and on its E-fracture face, in this and previous studies, represents the natural distribution of postsynaptic membrane molecules or was produced during tissue preparation. Most previous studies used aldehyde-fixed tissues, and because aldehydes fixed by chemical crosslinking, it is possible that fixation made molecules aggregate which were normally free to move in the plane of the membrane. Those previous studies which avoided chemical fixation still used relatively slow methods of freezing (2, 17), which may have left time, during cooling, for a membrane phase change to occur. Conceivably, this could have pushed the molecules into patterns that they do not normally assume. Nevertheless, the pattern was still visible in our hands when fresh, living tissue was quick-frozen with a machine which has measured freezing times of <2 ms and which clearly freezes faster than other methods because it produces much smaller ice crystals. Of course, the tissue frozen in this machine had still been subjected to the trauma of dissection, but the same pattern was also present when tissue was perfused through the heart with isotonic aldehyde fixatives before dissection and then quick-frozen.

In any case, regardless of whether the molecular order was present in life or formed only during tissue preparation, the pattern of the order should indicate something about the basic bonding tendencies of the molecules involved. The most striking feature of the pattern, on both the membrane surface and on the E face was the alignment of particles into double rows. Often these double rows were broken crosswise into dimers or tetramers. In some areas, the adjacent double rows tended to align themselves parallel to each other to form quadruple or larger linear aggregates, which were the patterns recognized in earlier freeze-fracture studies of this membrane (17, 56, 66). Possibly, all these paired patterns reflect the receptor's underlying tendency to form dimers in vitro, which is a well-known biochemical finding (43, 63).

Unfortunately, it has not been easy to see whether the receptors in adjacent rows are strictly in step, so that they form a square array, or whether they are staggered relative to each other, so that they establish true close-packing or hexagonal symmetry. The difficulty has been that the membrane surfaces on which they sit are often tilted relative to the electron beam and thus are viewed obliquely. (Stereomicroscopy has only recently become available and has not yet resolved this problem.) If the molecules formed a true square array, it would indicate that they tend to bond to four nearest neighbors, which in turn could suggest that they may be composed of four symmetrical subunits. This would fit some of the biochemical data on the number of subunits found in the whole molecule (42, 46, 63, 70). On the other hand, if adjacent rows are actually staggered, it would instead suggest that the receptor moelcule has a six-sided symmetry and tends to form a hexagonal lattice. This would fit with a hexagonal pattern of receptor packing that has been seen in

FIGURE 23 View of a freeze-etched synapse similar to Fig. 22, which was rotary-replicated instead of unidirectionally shadowed. Contrast is higher, because platinum highlights synaptic vesicles and a mitochondrion (*M*) in the axon and highlights filaments in the postsynaptic cytoplasm. × 25,000; so 2.5 cm = 1 μm.

FIGURE 24 Another freeze-etched and rotary-replicated synapse which was fractured more obliquely. The nerve (*N*) was not broken open, and instead the lacelike basal lamina in the cleft around the nerve was exposed. Also, the filaments that support the postsynaptic membrane were revealed more clearly. × 40,000; so 1 cm ≃ 0.25 μm.

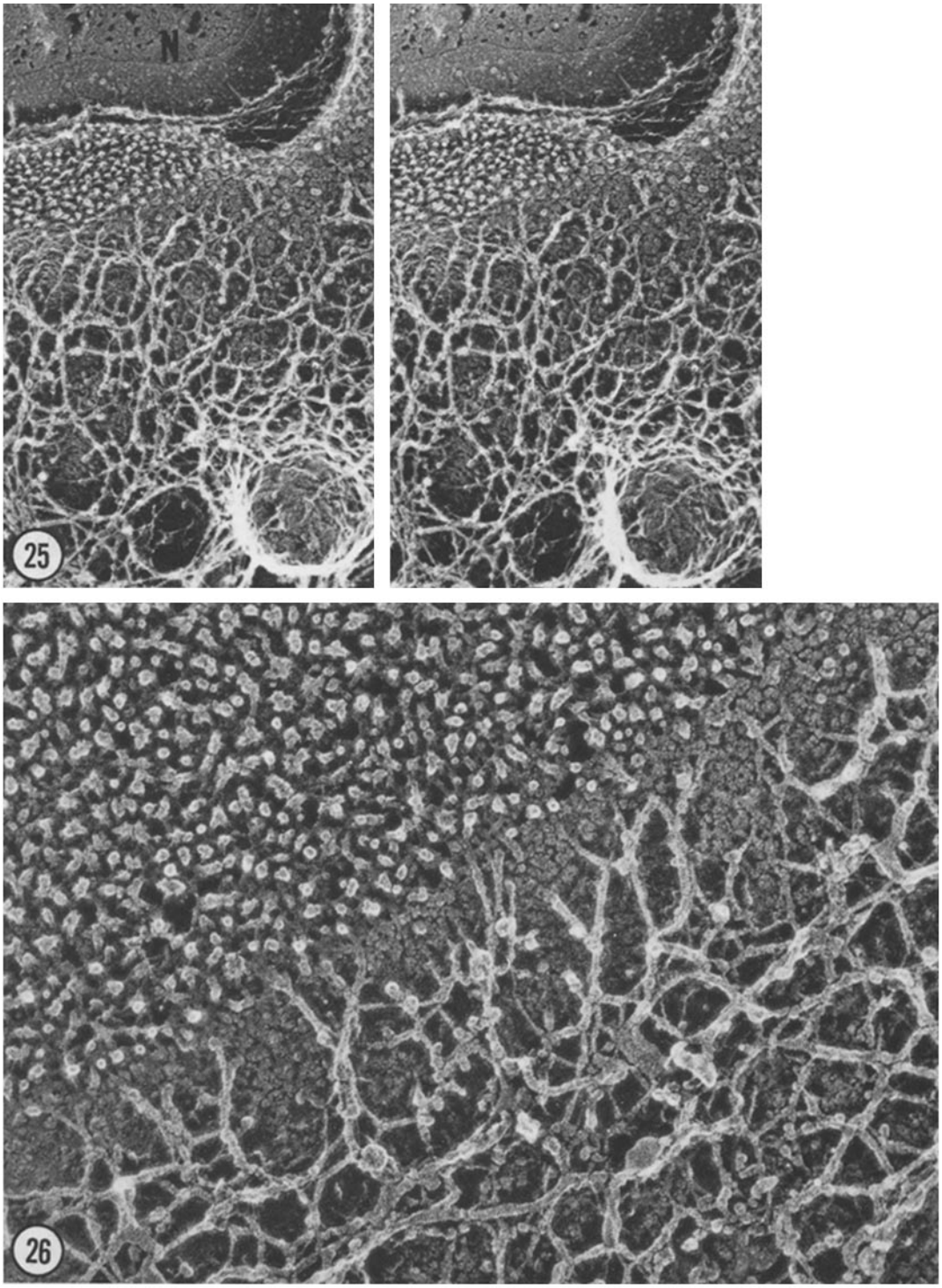

FIGURE 25 Stereo view of the underside of the postsynaptic membrane, in an area of an invagination (lower right), showing the loose mesh of cytoplasmic filaments which dangle from this surface. At the top is a bit of the nerve (*N*) on the far side of the synaptic cleft and then a small "speckly" area of E fracture-face. Interactions of cytoplasmic filaments with such surfaces are easier to see in such replicas than in the translucent images produced by high voltage electron microscopy. The rest is true inner surface. × 60,000; so 1 cm = 0.17 μm.

FIGURE 26 Higher magnification of the cytoplasmic filaments that appear to contact the underside of the postsynaptic membrane and, in the upper left, the rotary-replicated image of intramembrane particles on an E face that has partly collapsed because of deep-etching. × 133,000; so 1 mm = 7.5 nm.

negatively stained membrane fragments and has been focused on because it allowed optical diffraction to be done (17, 55, 67). However, hexagonal packing can also be created artifactually simply by pushing molecules forcefully together until they become close packed. This may well occur when postsynaptic membrane fragments are dried on grids and stained with heavy metals. For other reasons, too, postsynaptic membrane fragments may not be suitable for determining the native pattern of receptor packing. Brisson has shown that if such membrane fragments are left in a warm, oxidizing environment for several weeks, they display more and more hexagonally packed areas (J.-P. Changeux, personal communication).

Moreover, the pattern of aggregation seen in the postsynaptic membrane can in most cases be distinguished from the hexagonal crystallization that occurs in gap junctions when they become uncoupled (60). Here the intramembrane particles go from a random, loosely packed distribution in the coupled state into a tightly packed, obviously hexagonal lattice in the uncoupled condition (19, 30, 48, 60). The pattern of this crystallization characteristically begins with the formation of many small hexagonal aggregates which then appear to collapse into one large patch, thus strongly suggesting that the proteins that form the intramembrane particles develop a very high affinity for one another as soon as the junction is uncoupled (30). The pattern of the postsynaptic membrane is not so tight and is not so obviously hexagonal.

In fact, after all the methods of preparation used here, only portions of the membrane show any obvious pattern at all. Possibly this reflects that the receptors only barely express a tendency to interact with each other during life, and are constantly forming and dissolving small "crystallites" which hold together by hydrogen bonds or electrostatic bonds. This would be reminiscent of the currently favored model for the structure of liquid water (9, 28, 54), in which ordered clusters of molecules are thought to form and melt rapidly as a consequence of local energy fluctuations. These clusters, or microscopic "icebergs," are thought to be present in fully liquid water and to form a dynamic equilibrium with surrounding unbonded molecules which are free to move from cluster to cluster. If this were true also of the postsynaptic membrane, the ratio of clustered to unbonded receptors might depend on many factors, including temperature, ionic strength, concentration of receptors, and fluidity of the membrane. However, preliminary attempts to vary these parameters before quick-freezing the postsynaptic membrane, to test whether such a "liquid crystal" model (29, 31) could apply to the receptors in it, have so far not yielded obvious differences in the extent of patterned areas.

Interaction of the Membrane with Cytoplasmic and Extracellular Components

The receptor's tendency to organize in the plane of the membrane may help to explain how receptors first collect in the immediate postsynaptic area during development and how they stay put in the fully developed synapse. Initially, the embryonic postsynaptic cell is uniformly covered with receptors which are apparently free to diffuse randomly in the plane of the membrane (7, 26). Once it receives a nerve and begins to mature, it develops patches of high receptor concentration in the immediate vicinity of the nerve (5, 6, 59). The receptors in these areas are no longer free to diffuse away (7, 26) and are also slightly different biochemically (14). Perhaps this biochemical difference gives them an affinity for each other and leads to the growth of postsynaptic aggregates of receptors simply by gradual accretion. Once formed, such "rafts" of tethered receptors would naturally diffuse much more slowly in the plane of the membrane than would individual molecules, which could help to explain the stability of the postsynaptic receptor patch. However, such a simple view of receptor interaction does not explain why the crystallization would occur specifically beneath the nerve in the first place. The currently favored hypothesis to explain how this might occur is that the receptor aggregates become linked, either to stable cytoplasmic structures beneath the membrane (11, 24, 37) or to stable structures outside the cell, such as the basal lamina (50). The techniques introduced in this report permit the three-dimensional visualization of both such linkages.

The techniques illustrate that the cytoplasmic filaments which pervade the electrocyte contact the underside of the postsynaptic membrane directly. In addition, subsequent observations not detailed here indicate that when these filaments are dissolved by treatments which disrupt actin, the pattern of receptor packing in the postsynaptic membrane is also completely disorganized. However, there is no direct evidence yet that these

filaments are actin and no evidence that actin attaches directly to this membrane the way it does in other situations (51, 53, 69). Moreover, it is worth noting that *Torpedo* electric organ synapses do not display the pre- and postsynaptic "densities" which characterize most other synapses and which are thought to stabilize the synaptic membranes and link them to underlying cytoplasmic filaments (11, 22, 24).

Deep-etching and rotary-shadowing has also provided a high-resolution, scanning electron microscope-type view of the attachment of the basal lamina to the external surface of the postsynaptic membrane. Its attachments appear to be at least as abundant as the contacts of the underlying cytoplasmic filaments. Experimental evidence is gathering which suggests that the basal lamina may influence the distribution of receptors (50). It is one of the first differentiations to appear at developing synapses, even earlier than the cytoplasmic filaments beneath the postsynaptic membrane. It is known to bind the rich mass of acetylcholinesterase which is concentrated in the synaptic cleft during development (10, 18, 33, 47). Possibly, its attachments to the postsynaptic membrane are also able to "seed" the first crystallization of receptors that produces the "hot spots" beneath the arriving nerve (6).

It will be useful to observe embryonic or regenerating synapses with the techniques described here to learn more about how the pattern of postsynaptic membrane organization develops.

Thanks to Louise Evans for technical assistance, and to Anne Schneiderman, Harvard Neurobiology Department, for repeating the agonist and antagonist experiments while a student in the summer Neurobiology Course at the Woods Hole Marine Biology Laboratory.

Ms. Salpeter is currently a member of the class of 1982, University of California at San Francisco School of Medicine.

This work was supported by grants to Dr. Heuser from the United States Public Health Service (NS-11979) and the Muscular Dystrophy Association of America.

Received for publication 29 June 1978, and in revised form 6 February 1979.

REFERENCES

1. ABERMANN, R., M. M. SALPETER, and L. BACHMANN. 1972. High resolution shadowing. *In* Principles and Techniques of Electron Microscopy, Vol. 2. M. A. Hayat, editor. Van Nostrand Reinhold Company, New York, New York. 197–217.
2. ALLEN, T., R. BAERWALD, and L. T. POTTER. 1977. Postsynaptic membranes in the electric tissue of Narcine. II. A freeze-fracture study of nicotinic receptor molecules. *Tissue Cell.* **9**:595–608.
3. ALLEN, T., and L. T. POTTER. 1977. Postsynaptic membranes in the electric tissue of Narcine III. Isolation and Characterization. *Tissue Cell.* **9**:609–622.
4. ANDERSON, C. R., and C. F. STEVENS. 1973. Voltage clamp analysis of acetylcholine produced end-plate current fluctuations at frog neuromuscular junction. *J. Physiol. (Lond.).* **235**:655–692.
5. ANDERSON, M. J., and M. W. COHEN. 1974. Fluorescent staining of acetylcholine receptors in vertebrate skeletal muscle. *J. Physiol (Lond.).* **237**:385–400.
6. ANDERSON, M. J., and M. W. COHEN. 1977. Nerve-induced and spontaneous redistribution of acetylcholine receptors on cultured muscle cells. *J. Physiol. (Lond.).* **268**:757–773.
7. AXELROD, D., P. RAVDIN, D. E. KOPPEL, J. SCHLESSINGER, W. W. WEBB, E. L. ELSON, and T. R. PODLESKI. 1976. Lateral motion of fluorescently labeled acetylcholine receptors in membranes of developing muscle fibers. *Proc. Natl. Acad. Sci. U.S.A.* **73**:4594–4598.
8. BACHMANN, L., R. ABERMANN, and H. P. ZINGSHEIM. 1969. Improved Resolution in Freeze-etching. *Histochemie.* **20**:133–142.
9. BERNAL, J. D., and R. H. FOWLER. 1933. Theory of water and ionic solution, with particular reference to hydrogen and hydroxyl ions. *J. Chem. Phys.* **1**:515–548.
10. BETZ, W., and B. SAKMANN. 1973. Effects of proteolytic enzymes on function and structure of frog neuromuscular junctions. *J. Physiol. (Lond.).* **230**:673–688.
11. BLOMBERG, F., R. S. COHEN, and P. SIEKEVITZ. 1977. The structure of postsynaptic densities isolated from dog cerebral cortex. II. Characterization and arrangement of some of the major proteins within the structure. *J. Cell. Biol.* **74**:204–225.
12. BRANTON, D. 1966. Fracture faces of frozen membranes. *Proc. Natl. Acad. Sci. U.S.A.* **55**:1048–56.
13. BRANTON, D., S. BULLIVANT, N. B. GILULA, M. J. KARNOVSKY, H. MOOR, K. MÜHLETHALER, D. H. NORTHCOTE, L. PACKER, B. SATIR, P. SATIR, V. SPETH, L. A. STAEHELIN, R. L. STEERE, and R. S. WEINSTEIN. 1975. Freeze-etching nomenclature. *Science (Wash. D.C.).* **190**:54–56.
14. BROCKES, J. P., and Z. W. HALL. 1975. Acetylcholine receptors in normal and denervated rat diaphragm muscle. II. Comparison of junctional and extrajunctional receptors. *Biochemistry.* **14**:2100–2106.
15. BULLIVANT, D. 1977. Evaluation of membrane structure: facts and artifacts produced during freeze-fracture. *J. Microsc. (Oxf.).* **111**:101–116.
16. CARTAUD, J., and E. L. BENEDETTI. 1973. Presence of a lattice structure in membrane fragments rich in nicotinic receptor protein from the electric organ of *Torpedo marmorata*. *FEBS (Fed. Eur. Biochem. Soc.) Lett.* **33**:109–113.
17. CARTAUD, J., E. L. BENEDETTI, A. SOBEL, and J.-P. CHANGEUX. 1978. A morphological study of the cholinergic receptor protein from *Torpedo marmorata* in its membrane environment and in its detergent-extracted form. *J. Cell Sci.* **29**:313–337.
18. CARTAUD, J., S. BON, and J. MASSOULIE. 1978. Electrophorus acetylcholinesterase. Biochemical and electron microscope characterization of low ionic strength aggregates. *J. Cell Biol.* **77**:315–322.
19. CASPAR, D. L. D., D. A. GOODENOUGH, L. MAKOWSKI, and W. C. PHILLIPS. 1977. Gap junction structures. I. Correlated electron microscopy and x-ray diffraction. *J. Cell Biol.* **74**:605–628.
20. CLEMENTI, F., B. CONTI-TRONCONI, D. PELLUCHETTI, and M. MORGUTTI. 1975. Effect of denervation on the organization of the postsynaptic membrane of the electric organ of *Torpedo marmorata*. *Brain Res.* **90**:133–138.
21. COHEN, J. B., M. WEBER, M. HUCHET, and J.-P. CHANGEUX. 1972. Purification from *Torpedo marmorata* electric tissue of membrane fragments particularly rich in cholinergic receptor. *FEBS (Fed. Eur. Biochem. Soc.) Lett.* **26**:43–47.
22. COHEN, R. S., F. BLOMBERG, K. BERZINIS, and P. SIEKEVITZ. 1977. The structure of postsynaptic densities isolated from dog cerebral cortex. I. Overall morphology and protein composition. *J. Cell Biol.* **74**:181–203.
23. COULTER, H. D., and L. TERRACIOL. 1977. Preparation of biological tissues for electron microscopy by freeze-drying. *Anat. Rec.* **187**:477–493.
24. COUTEAUX, M. R., and M. PECOT-DECHAVASSINE. 1968. Particularities structurales du sarcoplasme sous-neural. *C.R. Acad. Sci. (Paris). D.* **266**:8–10.
25. DANIELS, M. P., and Z. VOGEL. 1975. Immunoperoxidase staining of α-bungarotoxin binding sites in muscle endplates shows distribution of acetylcholine receptors. *Nature (Lond.).* **254**:399–341.
26. EDIDIN, M., and D. FAMBROUGH. 1973. Fluidity of the surface of cultured muscle fibres. Rapid lateral diffusion of marked surface antigens. *J. Cell Biol.* **56**:27–37.
27. FERTUCK, H. C., and M. M. SALPETER. 1976. Quantitation of junctional and extrajunctional acetylcholine receptors by electron microscope autoradiography after ^{125}I-α-bungarotoxin binding at mouse neuromuscular junctions. *J. Cell Biol.* **69**:144–158.
28. FRANK, H. S. 1958. Covalency in the hydrogen bond and the properties

of water and ice. *Proc. R. Soc. Lond. A.* **247**:481–492.
29. FRIBERG, S., editor. 1976. Lyotrophic liquid crystals and the structure of biomembranes. 5th International Conference on Liquid Crystals, Stockholm. American Chemical Society, Wash. D.C.
30. GOODENOUGH, D., D. PAUL, and K. CULBERT. 1978. Correlative gap junction ultrastructure. *In* Birth Defects: Original Article Series. R. Lerner, editor. The National Foundation. Book IV. **2**:83–97.
31. GRAY, G. W. 1962. The molecular structure and the properties of liquid crystals. Academic Press Inc. (London) Ltd., London.
32. GROSS, H., E. BAS, and H. MOOR. 1978. Freeze-fracturing in ultrahigh vacuum at −196°C. *J. Cell Biol.* **76**:712–728.
33. HALL, Z. W., and R. B. KELLY. 1971. Enzymatic detachment of endplate acetylcholinesterase from muscle. *Nat. New Biol.* **232**:62–63.
34. HEUSER, J. E. 1976. Morphology of synaptic vesicle discharge and reformation of the frog neuromuscular junction. Chapter 3. *In* The Motor Innvervation of Muscle. S. Thesleff, editor. Academic Press Inc. (London) Ltd. London. 51–115.
35. HEUSER, J. E. 1977. Synaptic vesicle exocytosis revealed in quick-frozen frog neuromuscular junctions treated with 4-aminopyridine and given a single electrical shock. *In* Neuroscience Symposia, Volume 2. W. M. Cowan and J. A. Ferrendelli, editors. 215–239.
36. HEUSER, J. E., and A. M. LENNON. 1973. Morphological evidence for exocytosis of acetylcholine during formation of synaptosomes from *Torpedo* electric organ. *J. Physiol. (Lond.)* **233**:39–41P.
37. HEUSER, J. E., and T. S. REESE. 1977. Chapter 8. Structure of the synapse. *Handb. Physiol.* **1**:261–294.
38. HEUSER, J. E., T. S. REESE, M. J. DENNIS, L. Y. JAN, and L. EVANS. 1978. Synaptic vesicle exocytosis captured by quick-freezing and correlated with quantal transmitter release. *J. Cell Biol.* **81**:275–300.
39. HEUSER, J. E., T. S. REESE, and D. M. D. LANDIS. 1974. Functional changes in frog neuromuscular junctions studied with freeze-fracture. *J. Neurocytol.* **3**:109–131.
40. HEUSER, J. E., T. S. REESE, and D. M. D. LANDIS. 1976. Preservation of synaptic structure by rapid freezing. *Cold Spring Harbor Symp. Quant. Biol.* **40**:17–24.
41. KAMINER, B., and E. SZONYI. 1973. "Muscle" proteins in the electric organ of the Torpedo. *Biol. Bull. (Woods Hole).* **145**:441–442.
42. KARLIN, A., E. HOLTZMAN, R. VALDERRAMA, V. DAMLE, K. HSU, and F. REYES. 1978. Binding of antibodies to acetylcholine receptors in *Electrophorus* and *Torpedo* electroplax membranes. *J. Cell Biol.* **76**:577–592.
43. KARLIN, A., C. L. WEILL, M. G. MCNAMEE, and R. VALDERRAMA. 1975. Facets of the structures of acetylcholine receptors from *Electrophorus* and *Torpedo*. *Cold Spring Harbor Symp. Quant. Biol.* **40**:203–210.
44. KATZ, B., and R. MILEDI. 1972. The statistical nature of the acetylcholine potential and its molecular components. *J. Physiol. (Lond.)* **224**:665–699.
45. KISTLER, J., and E. KELLENBERGER. 1977. Collapse phenomena in freeze-drying. *J. Ultrastruct. Res.* **59**:70–75.
46. LINDSTROM, J., B. EINARSON, and J. MERLIE. 1977. Immunization of rats with polypeptide chains from *Torpedo* acetylcholine receptor causes an autoimmune response to receptors in rat muscle. *Proc. Natl. Acad. Sci. U.S.A.* **75**:769–773.
47. LWEBUGA-MUKASA, T. S., S. LAPP, and P. TAYLOR. 1976. Molecular forms of acetylcholinesterase from *Torpedo californica*, their relationship to synaptic membranes. *Biochemistry.* **15**:1425–1434.
48. MAKOWSKI, L., D. L. D. CASPAR, W. C. PHILLIPS, and D. A. GOODENOUGH. 1977. Gap junction structures. II. Analysis of the X-ray diffraction data. *J. Cell Biol.* **74**:629–645.
49. MARGARITIS, L. H., A. ELGASAETER, and D. BRANTON. 1977. Rotary replication for freeze-etching. *J. Cell Biol.* **72**:47–56.
50. MCMAHAN, U. J., J. R. SANES, and L. M. MARSHALL. 1978. Cholinesterase is associated with the basal lamina at the neuromuscular junction. *Nature (Lond.).* **271**:172–174.
51. MCNUTT, N. S. 1978. A thin-section and freeze fracture study of microfilament-membrane attachments in choroid plexus and intestinal microvilli. *J. Cell Biol.* **79**:774–787.
52. MISRA, D. N., and N. N. DAS GUPTA. 1965. Distortion in dimensions produced by shadowing for electron microscopy. *J. R. Micosc. Soc.* **84**:373–384.
53. MOOSEKER, M. S., and L. G. TILNEY. 1975. The organization of an actin filament-membrane complex: Filament polarity and membrane attachment in the microvilli of intestinal epithelial cells. *J. Cell Biol.* **67**:725–738.
54. NEMETHY, G., and H. A. SCHERAGA. 1962. Structure of water and hydrophobic bonding in proteins. A model for the thermodynamic properties of liquid water. *J. Chem. Phys.* **36**:3382–3400.
55. NICKEL, E., AND L. T. POTTER. 1973. Ultrastructure of isolated membranes of *Torpedo* electric tissue. *Brain Res.* **57**:508–517.
56. ORCI, L., A. PERRELET, and Y. DUNANT. 1974. A peculiar substructure in the postsynaptic membrane of *Torpedo* electroplax. *Proc. Natl. Acad. Sci. U.S.A.* **71**:307–310.
57. PEPER, K., F. DREYER, and K.-D. MULLER. 1975. Analysis of cooperativity of drug-receptor interaction by quantitative iontophoresis at frog motor end plates. *Cold Spring Harbor Symp. Quant. Biol.* **40**:187–193.
58. PEPER, K., F. DREYER, C. SANDRI, K. AKERT, and H. MOOR. 1974. Structure and ultrastructure of the frog motor endplate. A freeze-etching study. *Cell Tissue Res.* **149**:437–455.
59. PENG, H. B., and Y. NAKAJIMA. 1978. Membrane particle aggregates in innervated and noninnervated cultures of Xenopus embryonic muscle cells. *Proc. Natl. Acad. Sci. U.S.A.* **75**:500–504.
60. PERACCHIA, C. 1977. Gap junctions. Structural changes after uncoupling procedures. *J. Cell Biol.* **72**:628–641.
61. POPOT, J.-L., H. SUGIYAMA, and J.-P. CHANGEUX. 1976. Studies on the electrogenic action of acetylcholine with *Torpedo marmorata* organ. II. The permeability response of the receptor-rich membrane fragments to cholinergic agonists in vitro. *J. Mol. Biol.* **106**:469–483.
62. POTTER, L. T., and D. S. SMITH. 1977. Postsynaptic membranes in the electric tissue of *Narcine*: I. Organization and innervation of electric cells. Fine structure of nicotinic receptor-channel molecules revealed by transmission microscopy. *Tissue Cell.* **9**:585–594.
63. RAFTERY, M. A., R. L. VANDLEN, K. L. REED, and T. LEE. 1975. Characterization of *Torpedo californica* acetylcholine receptor: Its subunit composition and ligand-binding properties. *Cold Spring Harbor Symp. Quant. Biol.* **40**:193–202.
64. RASH, J. E., and M. H. ELLISMAN. 1974. Studies of excitable membranes. I. Macromolecular specializations of the neuromuscular junction and nonjunctional sarcolemma. *J. Cell Biol.* **63**:567–586.
65. RASH, J. E., C. S. HUDSON, and M. H. ELLISMAN. 1978. Ultrastructure of acetylcholine receptors at the mammalian neuromuscular junction. *In* Cell Membrane Receptors for Drugs and Hormones: A Multidisciplinary Approach. L. Bolis and R. W. Straub, editors. Raven Press, Inc., New York. 47–68.
66. ROSENBLUTH, J. 1975. Synaptic membrane structure in *Torpedo* electric organ. *J. Neurocytol.* **4**:697–712.
67. ROSS, M. J., M. W. KLYMKOWSKY, D. A. AGARD, and R. M. STROUD. 1977. Structural studies of a membrane-bound acetylcholine receptor from *Torpedo californica*. *J. Mol. Biol.* **116**:635–659.
68. SALPETER, M. M., and M. E. ELDEFRAWI. 1973. Sizes of end plate compartments, densities of acetylcholine receptor, and other quantitative aspects of neuromuscular transmission. *J. Histochem. Cytochem.* **21**:769–778.
69. SCHOLLMEYER, J. E., D. E. GOLL, L. G. TILNEY, M. MOOSEKER, R. ROBSON, and M. STROMER. 1974. Localization of α-actinin in nonmuscle material. *J. Cell Biol.* **63**(2, Pt. 2):304*a*. (Abstr.)
70. SOBEL, A., M. WEBER, and J.-P. CHANGEUX. 1977. Large-scale purification of the acetylcholine-receptor protein in its membrane-bound and detergent-extracted forms from *Torpedo marmorata* electric organ. *Eur. J. Biochem.* **80**:215–224.
71. WOLOSEWICK, J. J., and K. R. PORTER. 1976. Stereo high-voltage electron microscopy of whole cells of the human diploid line, WI-38. *Am. J. Anat.* **147**:303–324.